Biochemical Pharmacology 226 (2024) 116344

Contents lists available at ScienceDirect

Biochemical Pharmacology

journal homepage: www.elsevier.com/locate/biochempharm

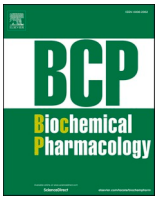

# A 14-amino acid cationic peptide Bolespleenin$_{334\text{-}347}$ from the marine fish mudskipper *Boleophthalmus pectinirostris* exhibiting potent antimicrobial activity and therapeutic potential

Yuqi Bai [a], Weibin Zhang [a], Wenbin Zheng [a], Xin-Zhan Meng [a], Yingyi Duan [a], Chang Zhang [a], Fangyi Chen [a,b,c,*], Ke-Jian Wang [a,b,c,*]

[a] State Key Laboratory of Marine Environmental Science, College of Ocean & Earth Sciences, Xiamen University, Xiamen, Fujian, China
[b] State-Province Joint Engineering Laboratory of Marine Bioproducts and Technology, College of Ocean & Earth Sciences, Xiamen University, Xiamen, Fujian, China
[c] Fujian Innovation Research Institute for Marine Biological Antimicrobial Peptide Industrial Technology, College of Ocean & Earth Sciences, Xiamen University, Xiamen, China

ARTICLE INFO

*Keywords:*
Mudskipper antimicrobial peptide
Bolespleenin$_{334\text{-}347}$
Membrane disruption
Superficial skin infection
MRSA

ABSTRACT

Antimicrobial peptides (AMPs) are an important component of innate immunity in both vertebrates and invertebrates, and some of the unique characteristics of AMPs are usually associated with their living environment. The marine fish, mudskipper *Boleophthalmus pectinirostris*, usually live amphibiously in intertidal environments that are quite different from other fish species, which would be an exceptional source of new AMPs. In the study, an AMP named Bolespleenin$_{334\text{-}347}$ was identified, which was a truncated peptide derived from a new functional gene found in *B. pectinirostris*, that was up-regulated in response to bacterial challenge. Bolespleenin$_{334\text{-}347}$ had only 14 amino acid residues, including five consecutive arginine residues. It was found that the peptide had broad-spectrum antibacterial activity, good thermal stability and sodium ion tolerance. Bolespleenin$_{334\text{-}347}$ killed *Acinetobacter baumannii* and *Staphylococcus aureus* by disrupting the structural integrity of the bacterial membrane, leading to leakage of the cellular contents, and inducing accumulation of bacterial endogenous reactive oxygen species (ROS). In addition, Bolespleenin$_{334\text{-}347}$ effectively inhibited biofilm formation of *A. baumannii* and *S. aureus* and long-term treatment did not lead to the development of resistance. Importantly, Bolespleenin$_{334\text{-}347}$ maintained stable activity against clinically multi-drug resistant bacterial strains. In addition, it was noteworthy that Bolespleenin$_{334\text{-}347}$ showed superior efficacy to LL-37 and vancomycin in a constructed mouse model of MRSA-induced superficial skin infections, as evidenced by a significant reduction in bacterial load and more favorable wound healing. This study provides an effective antimicrobial agent for topical skin infections with potential therapeutic efficacy for infections with drug-resistant bacteria, including MRSA.

## 1. Introduction

Antibiotics were one of the great discoveries of the 20th century, significantly reducing morbidity and mortality associated with infectious diseases, whose contribution to major advances in medicine has attracted much attention from the scientific community [1]. The two decades beginning in the 1940s were the golden age of antibiotic development, during which most antibiotics were discovered [2]. The ensuing explosion of misuse in medical and agricultural fields led to the rapid development of bacterial resistance [3]. Skin and soft tissue infections (SSTIs) are among the most common infections worldwide. They vary in severity from mild self-limiting superficial infections or life-threatening invasive infections [4]. Community and healthcare acquired SSTIs are most commonly caused by *Staphylococcus aureus* [5]. They present with a variety of symptoms, including impetigo, ecthyma, and cellulitis [6]. Superficial SSTIs may lead to invasive infections such

*Abbreviations:* AMPs, antimicrobial peptides; MRSA, methicillin-resistant *S. aureus*; SSTIs, skin and soft tissue infections; MIC, minimum inhibitory concentration; MBC, minimum bactericidal concentration; CFU, colony forming units; SEM, scanning electron microscopy; TEM, transmission electron microscopy; CLSM, confocal laser scanning microscopy; NPN, N-phenyl-L-naphthylamine; PMB, polymyxin B; TEWL, transepidermal water loss; ROS, reactive oxygen species; APD, antimicrobial peptide database.

* Corresponding authors at: State Key Laboratory of Marine Environmental Science, College of Ocean & Earth Sciences, Xiamen University, Xiamen, Fujian, China.
*E-mail addresses:* chenfangyi@xmu.edu.cn (F. Chen), wkjian@xmu.edu.cn (K.-J. Wang).

https://doi.org/10.1016/j.bcp.2024.116344
Received 7 February 2024; Received in revised form 4 June 2024; Accepted 6 June 2024
Available online 7 June 2024

as bacteremia and osteomyelitis [7]. Global epidemiologic data show an increasing incidence and severity of SSTIs associated with methicillin-resistant *S. aureus* (MRSA) [8]. Of the 422 patients with SSTI who participated in the clinical study, 76 % had *S. aureus* isolated, with MRSA prevalence as high as 59 % [9]. Skin infections are usually treated on an outpatient basis with oral antibiotics and topical care. Topical treatment strategies for MRSA include fusidic acid, but due to its widespread use, resistance is now evident [10]. Mupirocin, a therapeutic agent used for nasal colonization and skin infections, is effective against *S. aureus*, but its efficacy against MRSA infections is currently unclear [11]. Vancomycin is known to be the first-line therapy against MRSA infections and is usually used for topical or systemic treatment [12]. However, in clinical practice, it has to be used cautiously as the last line of defense against MRSA due to the development of resistance or nephrotoxicity caused by systemic therapy [13]. Not only MRSA, but drug-resistant bacterial infections are currently responsible for more than 700,000 deaths per year worldwide. This number is expected to surge to 10 million by 2050 [14]. The gravity of the situation has forced many countries to set strict regulations on the use of antibiotics in healthcare facilities and agriculture, and has called for an accelerated exploration of viable alternatives to antibiotics [15,16].

In comparison to conventional antibiotics, antimicrobial peptides (AMPs) offer novel opportunities for the treatment of infections, and their diverse mechanisms of action have additional potential. AMPs exhibit potent antibacterial, antifungal, antiviral, and even tumor inhibitory activities [17]. AMPs are mostly cationic peptides with an amphiphilic structure that target the bacterial membrane structures composed of anionic polysaccharides or lipids, which is paramount for membrane disruption [18]. In addition to their propensity to induce membrane disruption, many AMPs (e.g., the defensins and cathelicidins families) exhibit additional functional activities, including the modulation of inflammatory responses, which is crucial as uncontrolled inflammation has the potential to induce autoimmune diseases [19,20]. In addition, the chemotactic effect of AMPs is demonstrated by the recruitment of neutrophils, dendritic cells, T cells, and macrophages for bactericidal purposes [21]. With their high potency and selectivity, wide range of targets, potentially low toxicity, low accumulation in tissues, and tendency not to trigger drug resistance, AMPs are considered promising anti-infective drug candidates [22,23]. Due to the differences between the composition of mammalian cell membrane and bacterial membrane structures, AMPs tend to selectively kill bacteria while having good biocompatibility with mammalian cells [18]. More evidence suggests AMPs have greater therapeutic potential of AMPs against the current dilemma of treating MRSA infections [24,25]. In a previous study, AMPs from seven different sources showed strong activity against 15 clinical MRSA isolates [26]. Despite the large number of AMP-related patents filed, very few AMPs have received approval from the U.S. Food and Drug Administration (FDA) or the European Union's European Medicines Agency (EMA), which is mandatory for market entry and clinical use [27]. This is mainly due to the fact that preclinical studies are usually conducted in the absence of physiological conditions. This means that the effects of factors such as (i) physiological levels of relevant ions, (ii) high ionic strengths (due to high salt concentrations) and (iii) the presence of proteolytic enzymes and physiological barriers are often overlooked [22,28]. The recent therapeutic peptide dataset shows that nearly 70 drug candidates (including one AMP) received regulatory approval in March 2017, and as of 2019, 27 AMPs are in clinical trials [29]. To improve their in vivo efficacy, many studies have focused on modifying known AMPs to compensate for their stability deficiencies, such as the introduction of unnatural amino acids, cyclization, esterification, and combined nanoparticle delivery [30], but the discovery of novel, natural AMPs that combine potent activity and stability remains the prior foundation of optimization efforts.

The ocean accounts for 71 % of the earth's surface area. Its marine environment of high salt, high pressure, different pH and temperature has created a huge biodiversity foundation for drug discovery. Compared with invertebrates, marine fish of the phylum Chordata have an advanced immune system, in which AMPs play an important role in innate immunity against pathogens [31]. Fish-derived AMPs can be classified into five different families, including hepcidins, β-defensins, histone-derived peptides, cathelicidins, and piscidinsk (fish-specific AMP family). Interestingly, the amino acid composition of marine-derived AMPs preferred arginine and leucine compared to terrestrial organisms, which may be related to environmental stability or the uniqueness of marine pathogens [32]. As reported, marine fish-derived AMPs exhibit good MRSA therapeutic potential, e.g. Epinecidin-1 from grouper (*Epinephelus coioides*) was more effective than vancomycin in treating whole wound trauma in MRSA-infected mice, as evidenced by a reduction in the bacterial load and suppression of inflammatory responses [33]. Tilapia-derived Piscidin4 (TP4) has significant anti-MARA activity and is involved in immunomodulation and wound healing processes [34]. The ocean contains abundant fish resources (more than 30,000 fish species) and represent a "treasure trove" of natural active substances [35]. The exploration and utilization of fish-derived AMPs deserves further attention.

Mudskipper *Boleophthalmus pectinirostris* is a special marine fish that lives in an environment similar to that of amphibians, and the complex environment requires more innate immune factors to satisfy its basic defense needs. As reported, homologous comparison of sequencing data from mudskipper with the AMP database effectively screened out a large number of candidate AMPs, including hemoglobin-derived AMPs, amyloid AMPs, and the piscidin family, etc [36], which fully demonstrated that mudskipper contains abundant AMP resources. However, this method has certain limitations and is not applicable to the identification of novel AMPs. In this study, we focused on the immune response genes after bacterial infection in mudskippers based on the previously established transcriptome library, and identified a novel functional gene from the differentially expressed genes, named *Bolespleenin*. Based on bioinformatics predictions and experimental validation, the truncated peptide Bolespleenin$_{334\text{-}347}$ was determined to have significant antibacterial activity. We explored its antibacterial mechanism, evaluated its properties in terms of bacterial resistance, and then constructed a mouse model of superficial skin infection caused by MRSA to evaluate its therapeutic potential. This study will enrich the repertoire of fish-derived AMPs and provide an ideal anti-infective agent candidate for the treatment of drug-resistance bacteria.

## 2. Materials and methods

### 2.1. Experimental strain

The standard strains used in this study were purchased from the China General Microorganism Culture Collection Center, including *Acinetobacter baumannii* (CGMCC no. 1.6769), *Pseudomonas aeruginosa* (CGMCC no. 1.2421), *Escherichia coli* (CGMCC no. 1.2389), *Edwardsiella tarda* (CGMCC no. 1.1872), *Aeromonas hydrophila* (CGMCC no. 1.2017), *Vibrio alginolyticus* (CGMCC no. 1.1833), *Staphylococcus aureus* (CGMCC no. 1.2465), *Staphylococcus epidermidis* (CGMCC no. 1.4260), *Listeria monocytogenes* (CGMCC no. 1.10753), *Enterococcus faecalis* (CGMCC no. 1.2135), *Corynebacterium glutamicum* (CGMCC no. 1.1886), *Bacillus cereu* (CGMCC no. 1.3760), *Crytococcus neoformans* (CGMCC no. 2.1563), *Candida albicans* (CGMCC no. 2.2411), *Fusarium oxysporum* (CGMCC no. 3.6785), *Fusarium solani* (CGMCC no. 3.5840), and *Aspergillus flavus* (CGMCC no. 3.4410). Additionally, clinically drug-resistant strains including MDR *A. baumannii* QZ18050, MDR *A. baumanni* QZ18055, MDR *P. aeruginosa* QZ19121, MDR *P. aeruginosa* QZ19122, MRSA QZ19130, MRSA QZ19134, were kindly provided by the Second Affiliated Hospital of Fujian Medical University (Quanzhou, Fujian, China). Fungal strains were cultivated in potato dextrose agar (Hope Bio, Qingdao, China) at 28 °C. Vibrio strains were propagated in marine broth 2216 medium agar (BD DIFCO, USA) at 28 °C, and the other strains were cultured in nutrient broth medium (OXBID, UK) at 37 °C.

### 2.2. Gene cloning of Bolespleenin

Mudskippers *B. pectinirostris* were obtained from the aquaculture base in Xiapu (Fujian, China). Tissue samples were collected, including liver, blood, spleen and kidney. Samples were treated with TRIzol reagent (Invitrogen, UK) following the manufacturer's instructions to extract total RNA. The concentration and quality of the extracted RNA were assessed using the Agilent 2100 bioanalyzer (Agilent Technologies, USA). To further ensure RNA integrity, agarose gel electrophoresis was employed. RNA samples from each tissue were mixed, reverse transcribed for cDNA using the SMARTer® RACE 5′/3′ Kit User Manual (Clontech, USA), and the full-length cDNA was amplified using long fragment high-fidelity enzyme LA Taq (Takara, Japan) according to the standard procedure of the instruction manual. The products were recombined into the pMD18-T vector (Takara, China) and sequenced by Sangon Biotech Co., Ltd (Shanghai, China).

### 2.3. Sequence analysis and truncated peptide synthesis

After gene cloning, a new functional gene was obtained and named *Bolespleenin*. Sequence identity prediction of this gene was performed using the NCBI online server (https://www.ncbi.nlm.nih.gov). Protein physicochemical properties were predicted using the ProtParam tool (https://web.expasy.org/protparam/) and HeliQuest tool (https://heliquest.ipmc.cnrs.fr/cgi-bin/ComputParams.py). The chemical structures of the peptides were generated employing Chemdraw (https://www.perkinelmer.com/category/chemdraw). Three-dimensional protein structure predictions were conducted using AlphaFold (https://github.com/deepmind/alphafold), and visualized by PyMOL software (https://www.pymol.org). AMP segmentation prediction was performed via the $CAMP_{R4}$ online website (http:// https://www.camp.bicnirrh.res.in/predict/).

The truncated peptide $Bolespleenin_{334\text{-}347}$ (H-LIGLYLLHRRRRRH-OH) derived from *Bolespleenin* was predicted to be a potential AMP and was subjected to solid-phase chemical synthesis by Genscript (Nanjing, China), with a purity of 96.67 % determined by reversed-phase high-performance liquid chromatography (RP-HPLC). The observed molecular weight was determined to be 1728.45 by electrospray ionisation mass spectrometry (ESI-MS). The synthesized peptides were stored in lyophilized form at a temperature of −80 °C.

### 2.4. Antimicrobial activity assay

The antimicrobial activity of $Bolespleenin_{334\text{-}347}$ was assessed using the micro broth dilution method as previously described [37]. Bacteria in logarithmic growth phase were harvested and diluted to $1 \times 10^6$ CFU/mL in Mueller-Hinton broth (MHB, Oxoid, UK). Subsequently, various concentrations of the peptides were prepared in 96-well polystyrene flat-bottomed plates (NEST, China) using Milli-Q water and introduced into the bacterial suspensions. The final concentrations of peptides ranged from 1.5 to 96 μM (conventional antibiotic control LL-37 purchased from GL Biochem, Shanghai, China). Control wells consisted of bacterial suspensions treated with Milli-Q water only. The co-incubation plates were maintained at the optimal growth temperature for the respective bacteria and incubated for 24 h. The minimum inhibitory concentration (MIC), corresponding to the lowest peptide concentration that completely inhibit bacterial growth as visually determined, and the minimum bactericidal concentration (MBC), which represents the lowest peptide concentration required to kill 99.9 % of the microorganisms, were determined through colony counting. Three replicates were set up for each of the three independent experiments.

### 2.5. Measurement of peptide thermal stability and sodium ion tolerance

Peptide stability was assessed following the established methodology detailed in previous literature [38]. Briefly, *A. baumannii* and *S. aureus* cultures in their logarithmic growth phase were harvested and diluted to an approximate concentration of $1 \times 10^6$ CFU/mL. Subsequently, $Bolespleenin_{334\text{-}347}$ was heat-treated in a controlled water bath at 100 °C for 10, 20 and 30 min, respectively. After cooling, the peptide was mixed with diluted bacterial suspension in microtiter plate wells and maintained at 37 °C. Absorbance values at a wavelength of 600 nm were read at predefined intervals using an enzymatic microplate reader (Infinite F200 PRO, Tecan, Switzerland). Three replicates were set up for each of the three independent experiments.

To assess sodium ion tolerance, diluted bacterial solutions were co-incubated with peptide solutions containing different concentrations of NaCl (10 to 500 mM) in microtiter plate wells for 1 h at 37 °C in a constant temperature incubator. Subsequently, the bacterial solutions were taken for plate counting. Three replicates were set up for each of the three independent experiments.

### 2.6. The time killing kinetics

For time-dependent bactericidal kinetics assessment, *A. baumannii* and *S. aureus* were suspended in MHB to a concentration of approximately $1 \times 10^6$ colony-forming units per milliliter (CFU/mL). Incubation with 3 μM $Bolespleenin_{334\text{-}347}$ was initiated, and aliquots were taken at specific time intervals for assessment. The aliquots were plated onto nutrient broth (NB, HKM, China) agar plates, followed by an incubation of 18–24 h at 37 °C. After incubation, viable colonies were counted. The percentage of viable colonies (%CFU) at each time point was calculated as %CFU = (viable colonies at a specific time point / initial viable colonies) × 100 %. Three replicates were set up for each of the three independent experiments.

### 2.7. Electron microscope ultramicroscopy assay

The changes in the structure of bacterial membranes in the presence of $Bolespleenin_{334\text{-}347}$ were directly observed by scanning electron microscopy (SEM) according to established protocols [37,39]. Bacteria in the logarithmic growth phase were collected and suspended in NaPB buffer to a concentration of approximately $1 \times 10^7$ CFU/mL. A final concentration of 1 × MBC (3 μM) of $Bolespleenin_{334\text{-}347}$ was co-incubated with bacteria at 37 °C for 30 min. Subsequently, the bacteria were harvested by centrifugation (5000 g, 5 min), resuspended in 2.5 % (v/v) glutaraldehyde (Sigma, Germany) fixative and incubated at 4 °C overnight. After three washes, 10 μL NaPB buffer was added to obtain a high-concentration suspension. The suspension was then added dropwise onto pre-cut poly-L-lysine-coated slides (0.5 cm × 0.8 cm) and placed on ice for 30 min, then the excess liquid was removed by pipetting with filter paper, followed by critical point drying (EM CPD300, Leica, Germany) after dehydration in an ethanol gradient. The metal was sprayed with an ion sputter coater (JFC-1600, Jeol, Germany) and finally observed using a SEM (Zeiss SUPRA 55, Germany).

The internal structure of the bacteria was analyzed by transmission electron microscopy (TEM), and samples of $Bolespleenin_{334\text{-}347}$-treated bacteria were prepared following the same procedure as described above. The treated bacteria were embedded in 2 % agar blocks (2 mm × 2 mm), treated with 2.5 % glutaraldehyde overnight, washed with NaPB buffer, and then fixed with 1 % osmium tetroxide for 1 h. Afterwards, they were subjected to gradient dehydration with ethanol, stained with uranyl acetate, rinsed with acetone and embedded in epoxy resin. Ultrathin sections were prepared, and then visualized by TEM (HT-7800, Hitachi, Japan).

### 2.8. $Bolespleenin_{334\text{-}347}$ inhibited bacterial biofilm formation

The assessment of the effect on biofilm formation was performed following established methodology documented in previous studies [40]. Briefly, *A. baumannii* and *S. aureus* in logarithmic growth phase were collected, washed with NaPB and then diluted with MH medium to

a concentration of 1 × $10^6$ CFU/mL. The diluted bacteria were co-incubated with different final concentrations (0 to 48 μM) of Bolespleenin$_{334-347}$ in 96-well plates for 24 h. After incubation, the formed biofilm was stained with 0.1 % crystalline violet (CV, Sigma, Germany) and quantified by measuring the absorbance at 595 nm using an enzymatic microplate reader. Five replicates were set up for each independent experiment, for a total of three independent experiments.

### 2.9. Development of bacterial drug resistance under long-term stress of Bolespleenin$_{334-347}$

Based on previous studies with minor modifications, we assessed the development of resistance in *A. baumannii* and *S. aureus* under long-term treatment of Bolespleenin$_{334-347}$ [37]. Antibiotics involved in the experiments (including gentamicin, tigecycline, ampicillin, and vancomycin) were purchased from Sigma (Germany) and LL-37 was purchased from GL Biochem (Shanghai, China). Briefly, bacteria were harvested during the logarithmic growth phase and diluted in MHB to approximately 1 × $10^6$ CFU/mL. Selected antimicrobial agents (including Bolespleenin$_{334-347}$, LL-37 and selected traditional antibiotics) were used in antimicrobial assays, and the following day cultures were diluted 1,000-fold in sub-MIC concentration with fresh MHB, and the antimicrobial assay was repeated. The assay was carried out for 60 consecutive days using this approach and the change in MIC value was recorded. Three replicates were set up for each of the three independent experiments.

### 2.10. Localization of FITC-Labeled Bolespleenin$_{334-347}$ in bacteria

FITC-labeled Bolespleenin$_{334-347}$ was purchased from Genscript (Nanjing, China, purity 99.132 %, molecular weight 2362.0). According to the previous protocol with a slight modification [41], bacterial cultures from the mid-log phase were collected and suspended in PBS to reach an $OD_{600}$ of 0.1. Subsequently, FITC-labeled Bolespleenin$_{334-347}$ at different concentrations (3, 6, 12, and 24 μM) were co-incubated with the bacteria for 30 min, followed by three washes with PBS. The samples were then loaded into a 96-well glass-bottom plates (Cellvis P96 −1.5H-N) and examined under a confocal laser scanning microscopy (CLSM) with an excitation wavelength of 488 nm. The quantification of fluorescence intensity was conducted by Image J software.

### 2.11. Assessment of the permeability of bacterial outer and inner membranes in the presence of Bolespleenin$_{334-347}$

The altered permeability of the outer membrane of Gram-negative bacteria in the presence of Bolespleenin$_{334-347}$ was assessed using an N-phenyl-L-naphthylamine (NPN, Sigma, Germany) probe. Briefly, logarithmically harvested *A. baumannii* cells were suspended in HEPES buffer (pH 7.4, containing 5 mM glucose) and adjusted to a bacterial concentration of approximately 1 × $10^8$ CFU/mL. Subsequently, NPN was added at a final concentration of 10 μM. The bacteria-NPN mixture was introduced into a 96-well black flat-bottomed microtiter plate (NUNC, Roskilde, Denmark) and read at 350/420 nm using an enzymatic microplate reader until the background signal stabilized. Subsequently, different concentrations of Bolespleenin$_{334-347}$ (1.5 μM, 3 μM, 6 μM) were introduced into the wells with Milli-Q water as a negative control and 1 μg/mL polymyxin B (PMB) as a positive control. The changes in fluorescence signal were recorded at 2-minute intervals in each group, and three replicates were set up for each of the three independent experiments.

The effect of Bolespleenin$_{334-347}$ on the permeability of the bacterial inner membrane was assessed using the LIVE/DEAD BacLight™ kit (Thermo Fisher, USA) according to protocols previously reported [42]. Briefly, logarithmically growing *A. baumannii* and *S. aureus* cultures were collected, followed by three washes in 10 mM sodium phosphate buffer (NaPB, pH 7.4) to a density of 1 × $10^7$ CFU/mL. Bacterial suspensions were mixed with Bolespleenin$_{334-347}$ (6 μM) and co-incubated for 30 min at 37 °C. After two washes, SYTO 9 and PI were added for staining. Samples were incubated at room temperature for 15 min protected from light and then analyzed using CLSM (Zeiss LSM780, Germany) and a flow cytometer (Beckman CytoFlex, USA). The experiment was repeated three times independently.

### 2.12. Monitoring bacterial endogenous ROS in the presence of Bolespleenin$_{334-347}$

ROS levels induced by Bolespleenin$_{334-347}$ treatment of bacteria were quantified using the fluorescent probe 2′,7′-dichlorodihydrofluorescein diacetate (DCFH-DA) purchased from Nanjing Jiancheng Bioengineering Institute, Nanjing, China. *A. baumannii* and *S. aureus* were diluted to a concentration of 1 × $10^8$ CFU/mL in a solution of NaPB supplemented with 40 % MHB. The bacteria were then co-incubated for 30 min with various concentrations of Bolespleenin$_{334-347}$ (final concentrations of 1.5 μM, 3 μM, and 6 μM) or LL-37 at a final concentration of 12 μM. After washing three times with phosphate-buffered saline (PBS), DCFH-DA (final concentration of 10 μM) was introduced and incubated for another 30-minute. Finally, the fluorescence intensity was quantified using an enzymatic microplate reader with excitation/emission wavelengths at 488/525 nm. Five replicates were set up for each independent experiment, for a total of three independent experiments.

### 2.13. Evaluation of cytotoxicity and hemolytic activity of Bolespleenin$_{334-347}$

The cytotoxicity of Bolespleenin$_{334-347}$ was conducted using the MTS method according to the established protocol [37]. HEK-293 T (human embryonic kidney cell line) and HeLa (human cervical cancer cell line) were obtained from the Chinese Academy of Sciences Stem Cell Bank (https://www.cellbank.org.cn/), while ZF4 (zebrafish embryonic cell line) was obtained from the Institute of Hydrobiology, Chinese Academy of Sciences in Wuhan, China. These distinct cell lines were seeded into 96-well cell culture plates (Thermo Fisher, USA) at a density of 1 × $10^4$ cells/mL and cultured overnight in a 5 % $CO_2$ incubator (the optimal temperature was 37 °C for HEK-293 T and HeLa, and 28 °C for ZF4). After overnight incubation, the culture medium was replaced with fresh medium containing varying concentrations of the peptide (ranging from 0 to 48 μM) in each well. After24 hours of co-incubation, cell viability assay was performed using the CellTiter 96® AQueous kit (Promega, USA). Five replicates were set up for each of the three independent experiments.

The hemolytic potential of Bolespleenin$_{334-347}$ was assessed using freshly isolated mouse erythrocytes. The blood was subjected to centrifugation at 500g for 3 min, and the erythrocytes were then washed thoroughly with 0.9 % saline solution until the upper aqueous phase became clear. Subsequently, the erythrocytes were resuspended to a cell concentration of 4 %. In a 96-well plate, 100 μL of diluted erythrocyte suspension was co-incubated with 100 μL of each peptide concentration at 37 °C for 1 h. After co-incubation, the mixture was centrifuged at 4,000 rpm for 3 min, and the resulting supernatant was carefully collected in a new 96-well plate. The hemoglobin content was quantified by measuring the absorbance at 540 nm using an enzymatic microplate reader. Negative and positive controls were 0.9 % saline and 0.1 % Triton X-100/saline, respectively. The extent of hemolysis was calculated as follows: Hemolytic activity (%) = [($A_{540}$ of test sample−$A_{540}$ of negative control)] / ($A_{540}$ of positive control−$A_{540}$ of negative control) × 100 %. Four replicates were set up for each of the three independent experiments.

### 2.14. Therapeutic evaluation of Bolespleenin$_{334-347}$ against superficial skin infections in mice

Female BALB/c mice aged 6–8 weeks were purchased from the

Beijing Weitong Lihua Experimental Animal Technical Co., Ltd (Beijing, China). The animal protocols adhered to the Institutional Animal Care and Use Committee guidelines and received approval from the Ethics Committee of Xiamen University Laboratory Animal Center (XMULAC 20220128). Drawing on previous studies [11,43], mice were anesthetized by intraperitoneal injection of 2.5 % avertin (Sigma, Germany) solution and dorsally shaved. A superficial skin abrasion (including complete removal of the stratum corneum) was performed with sandpaper over an area of 1 $cm^2$. The effect of transepidermal water loss (TEWL) was assessed by Tewameter TM300 to measure the extent of skin barrier disruption (Courage and Khazaka). After that, the traumatized area was then inoculated with $1 \times 10^7$ CFU of MRSA QZ19130.

Follow-up administration was performed on all mice the following day, with 20 μL of the test substances (1 mg/mL of Bolespleenin$_{334\text{-}347}$, 1 mg/mL of LL-37, and 2 μg/mL of vancomycin) applied uniformly to the wound site once daily. Photographs were taken on days 1, 4, and 8 to document the progress of wound healing. Meanwhile, the body weights of the mice were recorded daily throughout the experimental period. On the 8th day, the mice were euthanized, and the traumatized skin was aseptically excised for subsequent bacterial load analysis and histopathological section evaluation.

### 2.15. Statistical analysis

The data was presented as mean ± standard deviations (SD). Statistical comparisons were performed using one-way analysis of variance (ANOVA) with SPSS 18.0 software. Differences were significant when the p-value was less than 0.05 ($P < 0.05$).

## 3. Result

### 3.1. Sequence analysis and truncated peptide prediction of Bolespleenin

The full-length cDNA sequence of *Bolespleenin* was obtained and has been included in the Genbank database. The gene contained a 76 bp 5′ untranslated region (5′ UTR) and a 315 bp 3′ UTR. Its open reading frame (ORF) encoded a protein containing 419 amino acids (GenBank accession no. OK432526). The protein had a predicted isoelectric point (pI) of 5.56 and a molecular weight of 45.7 kDa. Bioinformatics analysis of *Bolespleenin* was screened to obtain a potential AMP, a peptide consisting of 14 amino acid residues at the C-terminal end of the encoded protein named Bolespleenin$_{334\text{-}347}$ (H-LIGLYLLHRRRRRH-OH), which contained five consecutive arginines. As shown in Fig. 1, the tertiary structure of Bolespleenin$_{334\text{-}347}$ was predicted to be a typical α-helical structure with basic amino acids in the amino acid composition and protonatable groups (guanidyl and imidazole) on the side chain that can be hydrolyzed to provide cations. The physicochemical properties of Bolespleenin$_{334\text{-}347}$ indicate that it was an amphiphilic cationic peptide, with a predicted charge of + 5 and a hydrophobicity of 34.1 %. The AMP probability analysis was then performed based on the CAMP$_{R4}$ server, where the Random Forest (RF) model, Support Vector Machine (SVM), and the Artificial Neural Network (ANN) model predicted probabilities of 0.73, 0.98, and 0.94, respectively. All three models classified Bolespleenin$_{334\text{-}347}$ as an AMP.

### 3.2. Broad-spectrum antimicrobial activity of Bolespleenin$_{334\text{-}347}$

Antibacterial assays revealed the antibacterial spectrum of Bolespleenin$_{334\text{-}347}$ (LL-37 was used as a control for conventional antibiotics), as summarized in Table 1. Remarkably, the peptide exhibited stronger broad-spectrum antimicrobial activity than LL-37, where Bolespleenin$_{334\text{-}347}$ showed significant antimicrobial activity against Gram-negative bacteria (MIC ≤ 6 μM), such as *A. baumannii*, *P. aeruginosa*, and *E. coli*. Additionally, it also exhibited strong activity against common aquatic pathogens (3 μM ≤ MIC ≤ 24 μM), such as *A. hydrophila*, *E. tarda*, and *V. alginolyticus*. Moreover, most of the Gram-positive bacteria were susceptible to the peptide, with MIC values below 6 μM. In addition to bacteria, the peptide also effectively inhibited spore germination of fungi. The above results demonstrated the broad-spectrum antibacterial and antifungal activity of the peptide.

The efficacy of the peptide against clinically isolated drug-resistant bacteria was further assessed. Impressively, even at concentrations as low as 6 μM, Bolespleenin$_{334\text{-}347}$ showed significant inhibitory potential against drug-resistant variants of MDR *A. baumannii* (QZ18050, QZ18055), MDR *P. aeruginosa* (QZ19121, QZ19122), and MRSA (QZ19130, QZ19134).

### 3.3. Time-killing kinetics of Bolespleenin$_{334\text{-}347}$

The bactericidal efficiency of Bolespleenin$_{334\text{-}347}$ was assessed by bactericidal kinetics. The results showed that 3 μM Bolespleenin$_{334\text{-}347}$ was able to kill over 95 % of *A. baumannii* within 60 min. In contrast, it exhibited even more effective against *S. aureus*, achieving more than 95 % killing efficiency within 30 min (Fig. 2A).

### 3.4. Bacterial morphology changes after Bolespleenin$_{334\text{-}347}$ treatment

The bacterial surface structure was evaluated by scanning electron microscopy (SEM). As shown in Fig. 2B, the surface structure of the bacterial membrane in the control group was smooth without obvious damage. However, after treatment with 1 × MBC (3 μM) of Bolespleenin$_{334\text{-}347}$, the membrane surfaces of both *A. baumannii* and *S. aureus* showed obvious folds, which were severely manifested as holes and ruptures. Further ultrathin sectioning of the embedded bacterial samples and more detailed observation of the membrane structure and internal structure by transmission electron microscopy (TEM) showed that the

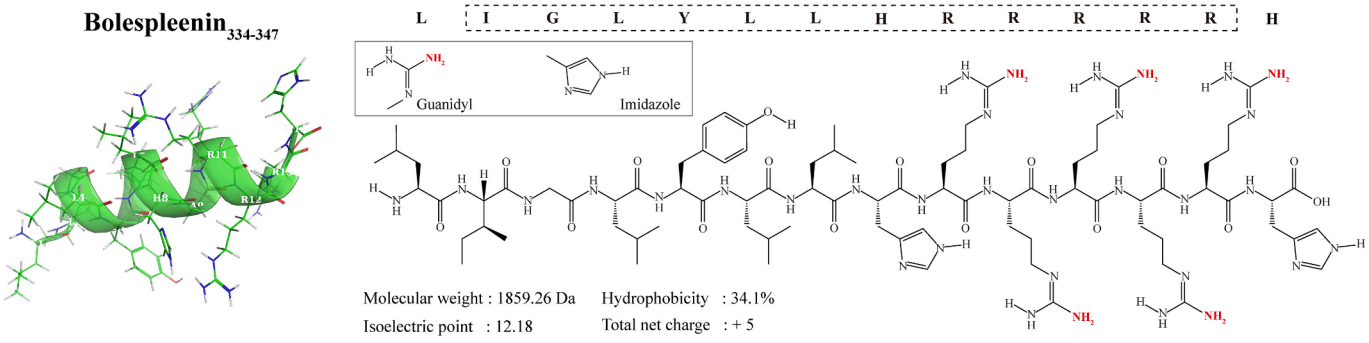


**Fig. 1. Analysis of the structure and physicochemical properties of Bolespleenin$_{334\text{-}347}$.** The three-dimensional structure of Bolespleenin$_{334\text{-}347}$ was predicted using AlphaFold; the α-helix constituting the amino acid in the structural formula is framed by a dashed line, and the structure contains basic side chains (guanidyl and imidazole), with positively charged groups labelled in red. (For interpretation of the references to colour in this figure legend, the reader is referred to the web version of this article.)

**Table 1**
Broad-spectrum antimicrobial assay for Bolespleenin$_{334-347}$.

| Strains | CGMCC NO[a] | MIC[b] (μM) | MBC[c]/MFC[d] (μM) | MIC (μM) |
|---|---|---|---|---|
| **Gram-negative bacteria** | **Bolespleenin$_{334-347}$** | | | **LL-37** |
| *Acinetobacter baumannii* | 1.6769 | 1.5–3 | 1.5–3 | 3–6 |
| *Pseudomonas aeruginosa* | 1.2421 | <1.5 | 1.5–3 | 6–12 |
| *Escherichia coli* | 1.2385 | 3–6 | 6–12 | 12–24 |
| *Aeromonas hydrophila* | 1.2017 | 12–24 | 24–48 | 48–96 |
| *Edwardsiella tarda* | 1.1872 | 12–24 | 12–24 | 48–96 |
| *Vibrio alginolyticus* | 1.1833 | 3–6 | 6–12 | 12–24 |
| **Gram-positive bacteria** | **Bolespleenin$_{334-347}$** | | | **LL-37** |
| *Staphylococcus aureus* | 1.2465 | <1.5 | 1.5–3 | 6–12 |
| *Staphylococcus epidermidis* | 1.4260 | <1.5 | <1.5 | 3–6 |
| *Listeria monocytogenes* | 1.10753 | 1.5–3 | 1.5–3 | 1.5–3 |
| *Enterococcus faecalis* | 1.2135 | 3–6 | 3–6 | 6–12 |
| *Corynebacterium glutamicum* | 1.1886 | <1.5 | <1.5 | <1.5 |
| *Bacillus cereu* | 1.3760 | 6–12 | 6–12 | <1.5 |
| **Fungi** | **Bolespleenin$_{334-347}$** | | | **LL-37** |
| *Crytococcus neoformans* | 2.1563 | <1.5 | <1.5 | 1.5–3 |
| *Candida albicans* | 2.2411 | 3–6 | 6–12 | 6–12 |
| *Fusarium oxysporum* | 3.6785 | 3–6 | 3–6 | 12–24 |
| *Fusarium solani* | 3.5840 | 3–6 | 3–6 | 6–12 |
| *Aspergillus flavus* | 3.4410 | 6–12 | 24–48 | 12–24 |
| **Multi-drug resistant bacteria[e]** | **Bolespleenin$_{334-347}$** | | | **LL-37** |
| MDR *A. baumannii* (QZ18050) | – | 1.5–3 | 3–6 | 3–6 |
| MDR *A. baumannii* (QZ18055) | – | 3–6 | 6–12 | 6–12 |
| MDR *P. aeruginosa* (QZ19121) | – | 3–6 | 6–12 | 6–12 |
| MDR *P. aeruginosa* (QZ19122) | – | 3–6 | 3–6 | 6–12 |
| MRSA (QZ19130) | – | 3–6 | 3–6 | 12–24 |
| MRSA (QZ19134) | – | 1.5–3 | 3–6 | 6–12 |

[a]China general microbiological culture collection center number. [b, c, d] Antimicrobial results were uniformly expressed in the A-B format, where A is the highest concentration at which visible microbial growth was observed in the experiment and B is the lowest concentration at which no microbial growth was observed in the experiment. [e] Multidrug-resistant strains isolated from clinical samples were provided by the Second Affiliated Hospital of Fujian Medical University (Quanzhou, Fujian, China).

bacteria exhibited cavitation after Bolespleenin$_{334-347}$ (1 × MBC) treatment, and fragments of the bacterial membrane structure and leaked contents were observed (Fig. 2C). Taken together, these results demonstrated that Bolespleenin$_{334-347}$ caused direct damage to the structure of the bacteria and might be an important cause of bacterial death.

### 3.5. Stability evaluation of Bolespleenin$_{334-347}$

The stability assessment of Bolespleenin$_{334-347}$ included the detection of its antimicrobial activity under different treatment conditions. As shown in Fig. 3A and C, exposure to 100 °C for 10 to 30 min had no significant effect on its activity. In addition, the effect of different sodium ion concentrations on its activity was evaluated. Results in Fig. 3B and D show that Bolespleenin$_{334-347}$ retained highly active at a concentration of 160 mM, reducing the number of viable bacteria by more than three orders of magnitude. Remarkably, at concentrations up to 200 mM, it remained effective against bacteria, although a substantial decrease in activity was observed. Temperature and ionic concentration are commonly used in the stability evaluation of AMPs, especially in certain diseases where high sodium ion concentration environments greatly limit the application of AMPs, and the above results demonstrated the good stability of Bolespleenin$_{334-347}$ under the tested conditions.

### 3.6. Anti-biofilm activity of Bolespleenin$_{334-347}$

Bacterial infections often culminate in the formation of biofilm structures, that exacerbate the challenges posed by antibiotic resistance [44]. The formation of biofilms greatly enhances bacterial resistance, leading to a surge in antibiotic tolerance ranging from 10 to 1000-fold [45]. In view of these concerns, our study analyzed the effect of different concentrations of Bolespleenin$_{334-347}$ (ranging from 3 μM to 48 μM) on the biofilm formation capacity of two pivotal pathogens (*A. baumannii* and *S. aureus*). The results showed a dose-dependent attenuation of the biofilm formation ability of both bacterial strains after Bolespleenin$_{334-347}$ treatment (Fig. 4A and B).

### 3.7. Antibacterial process of Bolespleenin$_{334-347}$ without inducing resistance

*A. baumannii* and *S. aureus* are common clinical pathogens that are rapidly developing resistance to conventional treatment [46]. In this study, we used two AMPs (Bolespleenin$_{334-347}$ and LL-37) and four conventional antibiotics for the evaluation of long-term resistance induction in two subject bacteria. Under 60 days of sub-MIC concentration stress, *A. baumannii* showed no significant changes in resistance to either AMP, compared to a more than 1,000-fold elevation in the gentamicin-treated group, and a more than 300-fold elevation in the tigecycline resistance was elevated (Fig. 4C). Neither AMPs induced resistance in *S. aureus* over a 60-day period, however, the MIC was elevated more than 400-fold in the ampicillin-treated group, and steadily increased approximately 5-fold in the vancomycin-treated group (Fig. 4D).

### 3.8. Bolespleenin$_{334-347}$ targets bacteria and disrupts outer membrane integrity

The membrane affinity of cationic peptides is highlighted by their selectivity for lipid membranes, with a predilection for bacterial membrane structures containing negatively charged phospholipids, thus promoting the accumulation of these cationic peptides [47]. In our study, Bolespleenin$_{334-347}$ was heavily enriched on the bacterial surface at a concentration of only 3 μM, and this enrichment showed a dose-dependent pattern (Fig. 5A to C).

The outer membranes of Gram-negative bacteria carry a large amount of anionic polysaccharides, that can limit the concentration of cationic peptides reaching the inner membrane [48]. Therefore, we here evaluated the integrity of the outer membrane of *A. baumannii* in the presence of Bolespleenin$_{334-347}$ by means of an NPN probe, which penetrates the damaged outer membrane of the bacterium and emits strong fluorescence upon binding to hydrophobic lipid. As shown in Fig. 5D, NPN fluorescence increased in a dose-dependent manner with increasing concentrations of Bolespleenin$_{334-347}$, reflecting increased permeability of the damaged outer membrane structure.

### 3.9. Bolespleenin$_{334-347}$ treatment increases bacterial inner membrane permeability

The effect of Bolespleenin$_{334-347}$ on the permeability of the bacterial inner membrane was evaluated by SYTO 9 and PI staining (Fig. 6A), in which SYTO 9 labeled all the bacteria, while PI can only pass through the damaged bacterial inner membrane and bind to its nucleic acids and emit red fluorescence, and the fluorescence co-localization was analyzed by CLSM. The results showed that for both bacteria tested, the bacterial inner membrane was intact in the control group, while almost all bacteria in the positive control group (PMB, 1 μg/mL) were labeled by the PI dye, implying that the bacterial inner membrane structure was severely damaged. Notably, after treatment with 1 × MBC (3 μM) of

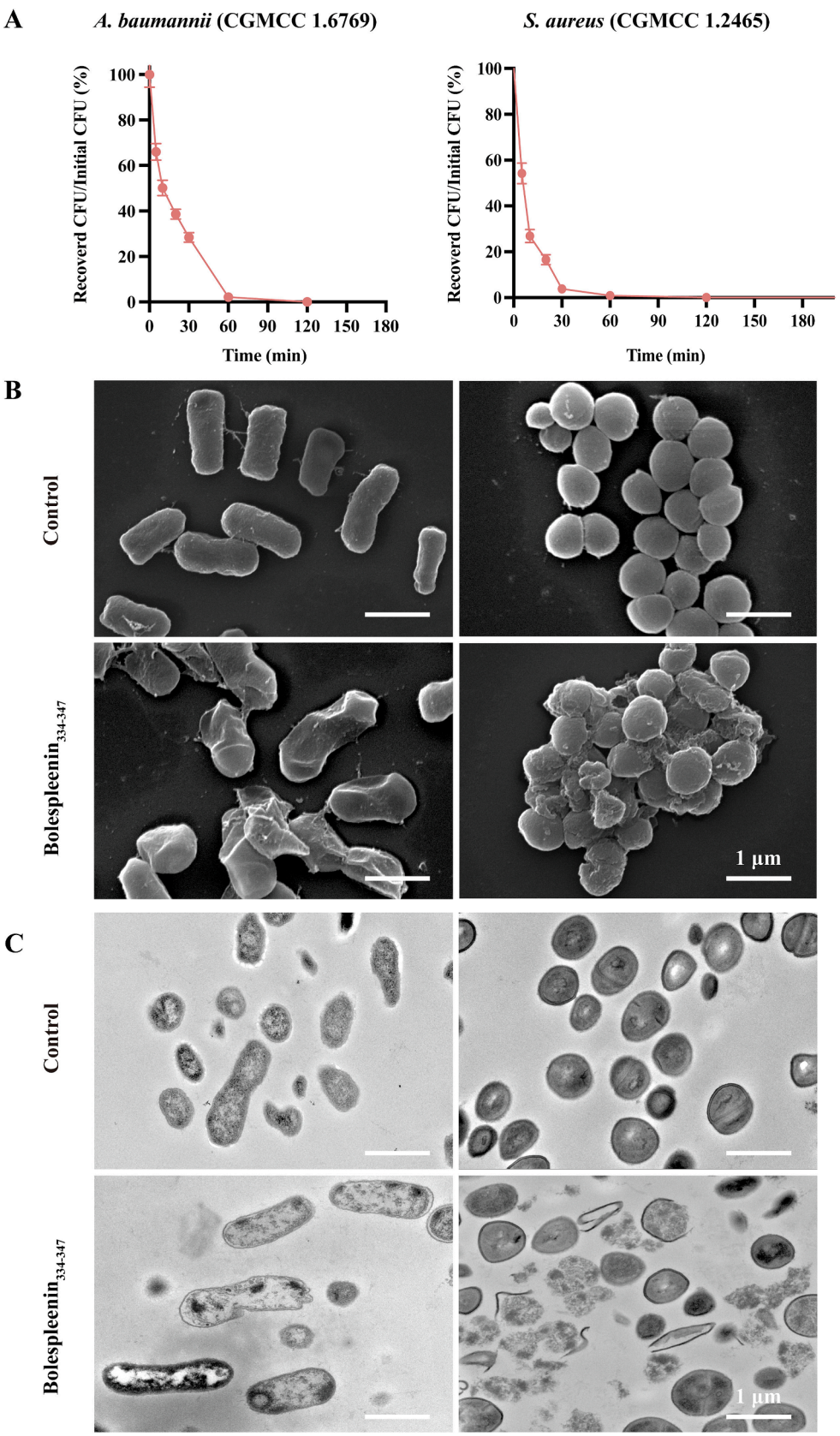


**Fig. 2. Bactericidal properties of Bolespleenin$_{334-347}$ against bacteria (*A. baumannii* and *S. aureus*, respectively).** (A) Time-dependent killing properties of Bolespleenin$_{334-347}$ against bacteria. (B) Structural changes of bacterial surface in the presence of Bolespleenin$_{334-347}$ as observed by SEM. (C) The embedded bacterial samples were sectioned and the bacterial structures were evaluated by TEM observation.

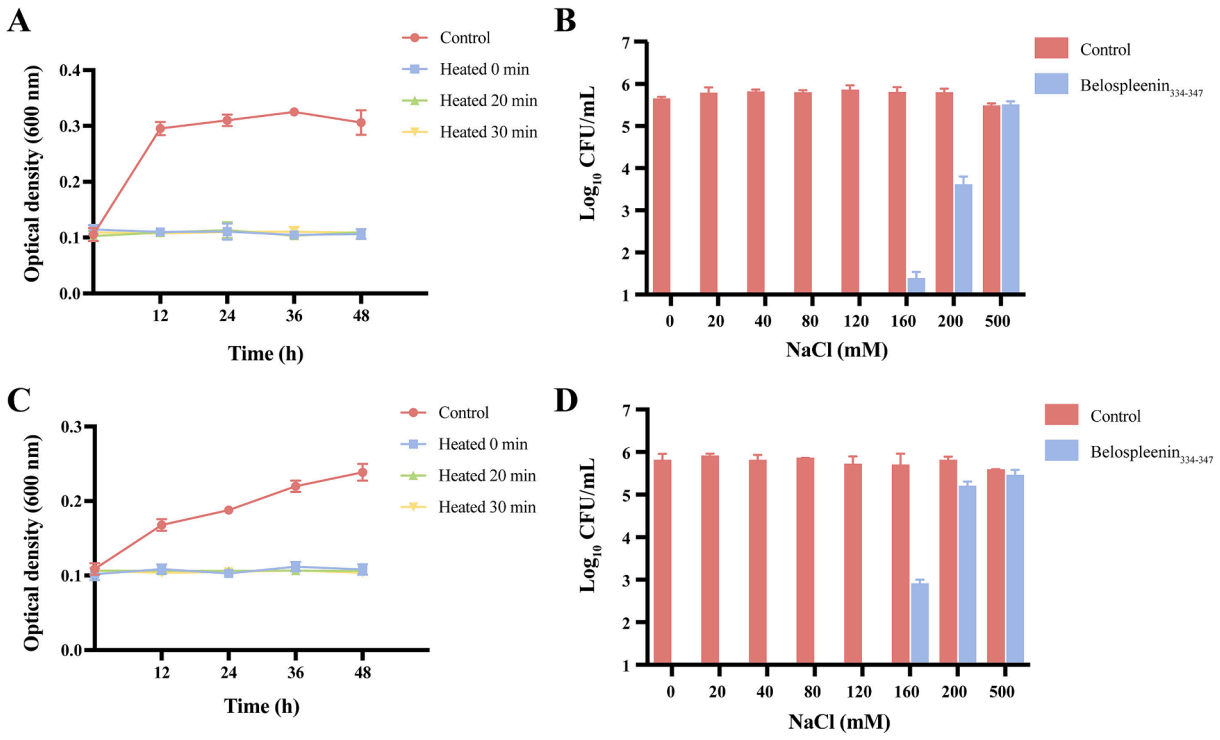


**Fig. 3. Stability evaluation of Bolespleenin$_{334-347}$.** The fluctuation of antimicrobial activity of Bolespleenin$_{334-347}$ against *A. baumannii* (A) and *S. aureus* (C) after high temperature treatment. The results were reflected by monitoring the $OD_{600}$ values during bacterial growth. The antimicrobial activity of Bolespleenin$_{334-347}$ against *A. baumannii* (B) and *S. aureus* (D) at different sodium ion concentrations.

Bolespleenin$_{334-347}$, a large amount of red fluorescent signals also appeared, suggesting that the permeability of the damaged bacterial endomembrane structure was increased. We further quantified the live-dead bacteria using flow cytometry (Fig. 6B), which showed that 1 μg/mL PMB led to the death of 78.2 % of the bacteria, while 3 μM Bolespleenin$_{334-347}$ resulted in 13.9 % bacterial death.

### 3.10. Increase in bacterial endogenous ROS after Bolespleenin$_{334-347}$ treatment

In the presence of antimicrobial agents, an increase in ROS excess due to oxidative stress is one of the major causes of bacterial death [49]. Endogenous ROS changes in the subject bacteria under the treatment of Bolespleenin$_{334-347}$ were monitored by DCFH-DA probe. The results showed that Bolespleenin$_{334-347}$ caused a significant and dose-dependent increase in endogenous ROS in *A. baumannii* at all three concentrations (1.5 μM, 3 μM, and 6 μM) as compared to the control (Fig. 7A). Similarly, for *S. aureus*, treatment with Bolespleenin$_{334-347}$ at 3 μM and 6 μM concentrations significantly increased endogenous ROS levels (Fig. 7B).

### 3.11. Bolespleenin$_{334-347}$ without cytotoxic and hemolytic activity

In addition to the stability of AMPs, the evaluation of their biocompatibility is an essential and critical part of the further application of AMPs [50]. In this study, we evaluated the cytotoxicity of Bolespleenin$_{334-347}$ *in vitro* using the mammalian cell line HEK-293 T, the cancer cell HeLa, and the fish cell line ZF4, with Melittin as a positive control (final concentration of 6 μM). As shown in Fig. 8A, none of the three cell lines exhibited significant cytotoxicity over the range of effective antimicrobial concentrations of Bolespleenin$_{334-347}$ (6 μM to 48 μM). In contrast, 6 μM Melittin showed significant cytotoxicity. We also evaluated the hemolytic activity of Bolespleenin$_{334-347}$ on mouse erythrocytes. Incubation of saline with erythrocytes as a negative control did not result in hemolysis, whereas 0.1 % Triton X-100 led to complete rupture of erythrocytes. Remarkably, no significant hemolysis was detected even when the concentration of Bolespleenin$_{334-347}$ was as high as 192 μM (as shown in Fig. 8B and C). These results demonstrated that Bolespleenin$_{334-347}$ had good biocompatibility.

### 3.12. Promotion of healing by Bolespleenin$_{334-347}$ in MRSA-induced superficial skin infections in mice

The experimental mice were subjected to superficial skin trauma, and the extent of epidermal trauma was determined by detecting wound water loss (pre-trauma TEWL value of 11.41 ± 6.81 g/m$^2$·h and post-trauma TEWL value of 67.20 ± 10.66 g/m$^2$·h), followed by topical inoculation of MRSA to complete the model construction. Photographs were taken to document wound recovery during the 8-day treatment period (Fig. 9A), and wound samples were collected on day 8 for bacterial load analysis and pathology section analysis (Fig. 9B and C). The results showed that the wound recovery was faster in the uninfected control (NC) group, with the stratum corneum returning to pre-traumatic levels. In contrast, wound healing showed impairment in the saline-treated group, with pathology sections showing dermal hemorrhage (indicated by red arrows) and edema (indicated by green arrows), and abnormal keratinization of the stratum corneum (indicated by black arrows). Of all three treatment groups, the Bolespleenin$_{334-347}$-treated group demonstrated the closest degree of wound healing to that of the NC group, with substantial restoration of keratinization, while the LL-37-treated group showed only a certain degree of keratinization insufficiency. In contrast, the vancomycin-treated group remained red and swollen on day 8, and pathological sections showed dermal edema and abnormal keratinization. Analysis of the bacterial load in each group showed that all three treatment groups had significantly lower bacterial loads than the saline-treated group. Notably, the reduction in bacterial load was significantly higher in the Bolespleenin$_{334-347}$-treated group than in the vancomycin-treated group. In addition, the body weights of the mice were monitored throughout the treatment phase, and the results showed a decreasing trend of body weights in all groups,

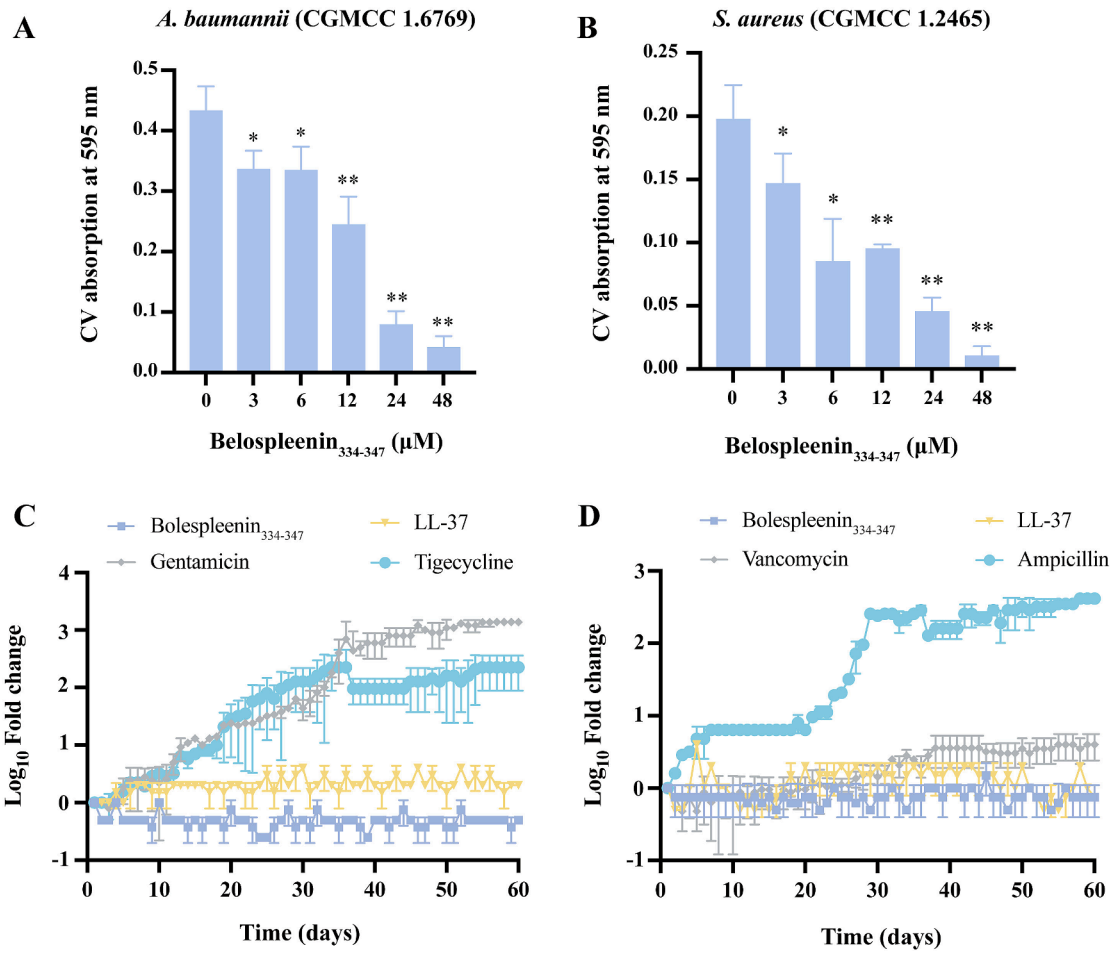


**Fig. 4. Bolespleenin$_{334-347}$ inhibits the development of adaptive resistance in bacteria.** Quantification of the impact of varying concentrations of Bolespleenin$_{334-347}$ on biofilm production in *A. baumannii* (A) and *S. aureus* (B) by measuring absorbance at 595 nm after CV staining. Data are presented as mean ± standard error of mean (n = 5). Statistical analysis was conducted through one-way ANOVA followed by the Dunnett post hoc test. * $p < 0.05$, ** $p < 0.01$. The elevation of drug resistance in *A. baumannii* (C) and *S. aureus* (D) is depicted by the fold change of MIC after prolonged exposure to subtherapeutic concentrations. The y-axis represents the fold change ($log_{10}$ scale) of MIC relative to day one, while the x-axis denotes the number of days (bacteria undergo one generation per day). The experiment was conducted in triplicate.

with more pronounced decreases in the vancomycin-treated and saline-treated groups (Fig. 9D). Overall, Bolespleenin$_{334-347}$ showed superior therapeutic effects to LL-37 and vancomycin in the treatment of MRSA-induced localized superficial skin infections.

## 4. Discussion

Nearly half of the AMPs included in the Antimicrobial Peptide Database (APD) are derived from amphibians, whose innate immunity has evolved unique adaptations under the selection pressures of complex living environments [51]. Mudskippers *B. pectinirostris* are amphibious fish that live in the intertidal zone, and possess a range of specific physiological characteristics to adapt to the complex environment between the sea and the land [52]. In this unique ecosystem, mudskippers need to cope with an underwater environment at high tide and a terrestrial environment at low tide [53]. Due to this complex living environment, mudskippers are under pressure from a wide variety of pathogenic microorganisms, and thus broad-spectrum antimicrobial activity is a necessary characteristic of AMPs from this species [36]. In addition, mudskippers are frequently subjected to changes in environmental factors such as tides, salinity and temperature, which contribute to the diversification of their AMPs and their high resistance to remain active under different conditions [54]. Previous studies have identified a variety of active substances in mudskipper that are directly involved in antimicrobial activity, including proteases, lectins, lysozymes, and AMPs [36,55,56]. In the study, a number of potential AMP genes were predicted by screening the transcriptomes of bacterially infected mudskippers previously established in our laboratory, some of which are highly homologous to AMPs in the APD database and the rest of which are novel. Among them, we focused on the novel functional gene, named *Bolespleenin,* which was significantly up-regulated after bacterial infection, and encoded a cationic peptide, Bolespleenin$_{334-347}$, consisting of 14 amino acid residues with five consecutive arginine residues. The cationic amphiphilic physicochemical properties of Bolespleenin$_{334-347}$ were predicted to have antimicrobial potential, and its broad-spectrum antimicrobial activity was further confirmed. Cationic AMPs usually bind to negatively charged polysaccharides and phospholipids in microbial membrane structures, selectively targeting and causing damage [57]. Bolespleenin$_{334-347}$ is predicted to have an α-helical structure, but membrane-active peptides are usually unstructured in aqueous solution, whereas in the presence of lipid membranes, they exhibit an α-helical structure, which leads to disruption of the bilayer structure [58]. Notably, Bolespleenin$_{334-347}$ contains a unique polyarginine sequence. In terms of amino acid composition, the basic amino acids arginine and lysine are both protonated to provide the positive charge, which is essential for the antimicrobial activity of the cationic peptides [59–61]. In addition, the unique guanidinium-based side chain of arginine forms a more stable structure with membrane components and typically

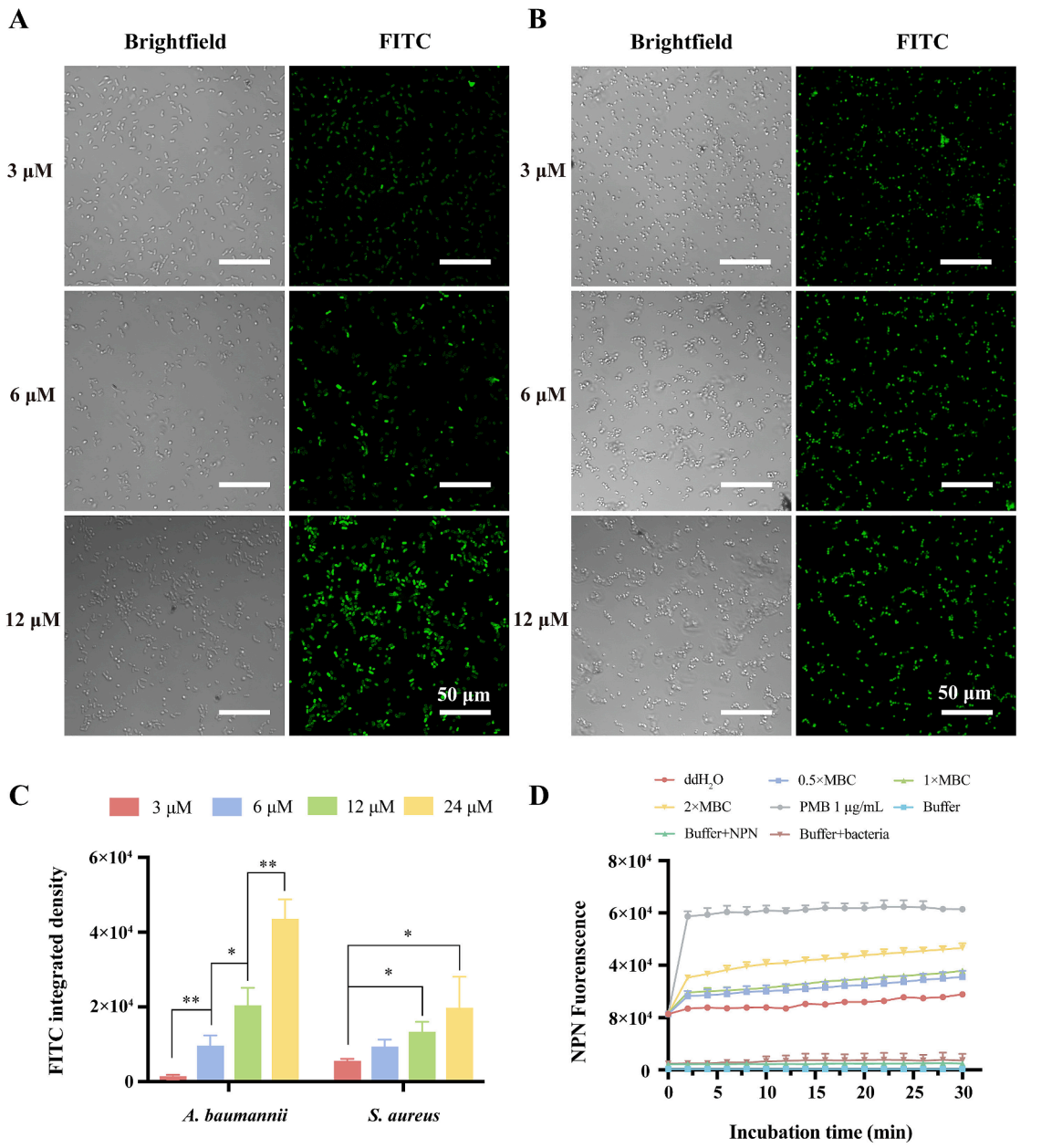


**Fig. 5. Bolespleenin$_{334\text{-}347}$ selectively targets bacterial membranes and disrupts outer membrane integrity.** (A) Co-localization of FITC-labeled Bolespleenin$_{334\text{-}347}$ in *A. baumannii* at 3 μM, 6 μM and 12 μM concentrations. (B) Co-localization of FITC-labeled Bolespleenin$_{334\text{-}347}$ in *S. aureus* at 3 μM, 6 μM and 12 μM concentrations. (C) Quantification of the fluorescence intensity and significance analysis by Image J software. Data are presented as mean ± standard error of mean (n = 3). Statistical analysis was conducted through one-way ANOVA followed by the Dunnett post hoc test. * $p < 0.05$, ** $p < 0.01$. (D) Outer membrane permeability after Bolespleenin$_{334\text{-}347}$ treatment. The NPN fluorescence was recorded at $\lambda_{ex}$ = 350 nm and $\lambda_{em}$ = 420 nm.

exhibits greater membrane perturbation than lysine, an advantage that is even more pronounced in the polyarginine structures [62,63].

Disruption of bacterial membrane structure is one of the bactericidal mechanisms of AMPs, which usually depends on the concentration of peptides on the membrane surface and leads to membrane structural disruption when a certain threshold is reached [64]. In this study, it was observed that Bolespleenin$_{334\text{-}347}$ co-localized on bacteria in a dose-dependent manner, and assessment of the structural integrity of the bacterial membranes showed that the permeability of both the outer and inner bacterial membranes was altered in the presence of Bolespleenin$_{334\text{-}347}$, and that the increase in permeability might lead to osmotic imbalance, which could interfere with normal physiological processes in bacteria. This result was consistent with electron microscopic observations that the surface of the bacterial membrane wrinkled or even ruptured in the presence of Bolespleenin$_{334\text{-}347}$, and leakage of bacterial contents was observed. In addition, we found a significant increase in bacterial endogenous ROS with treatment of Bolespleenin$_{334\text{-}347}$, indicating that the action of Bolespleenin$_{334\text{-}347}$ simultaneously triggered oxidative stress, and the excessive ROS may damage bacterial proteins, lipids, and DNA, leading to fatal bacterial damage [65,66]. Taken together, the disruption of membrane structure and the surge of ROS may act together in the bacterial killing process.

Biofilms are a survival strategy for bacteria to cope with environmental stresses and resist the action of antibiotics or other drugs [67]. Bacterial biofilm formation typically involves three stages: (i) planktonic phase, (ii) initial attachment to surfaces, and (iii) formation of microcolonies and secretion of extracellular polymeric substances (EPS). Once a dense EPS matrix is formed, it inhibits the penetration of

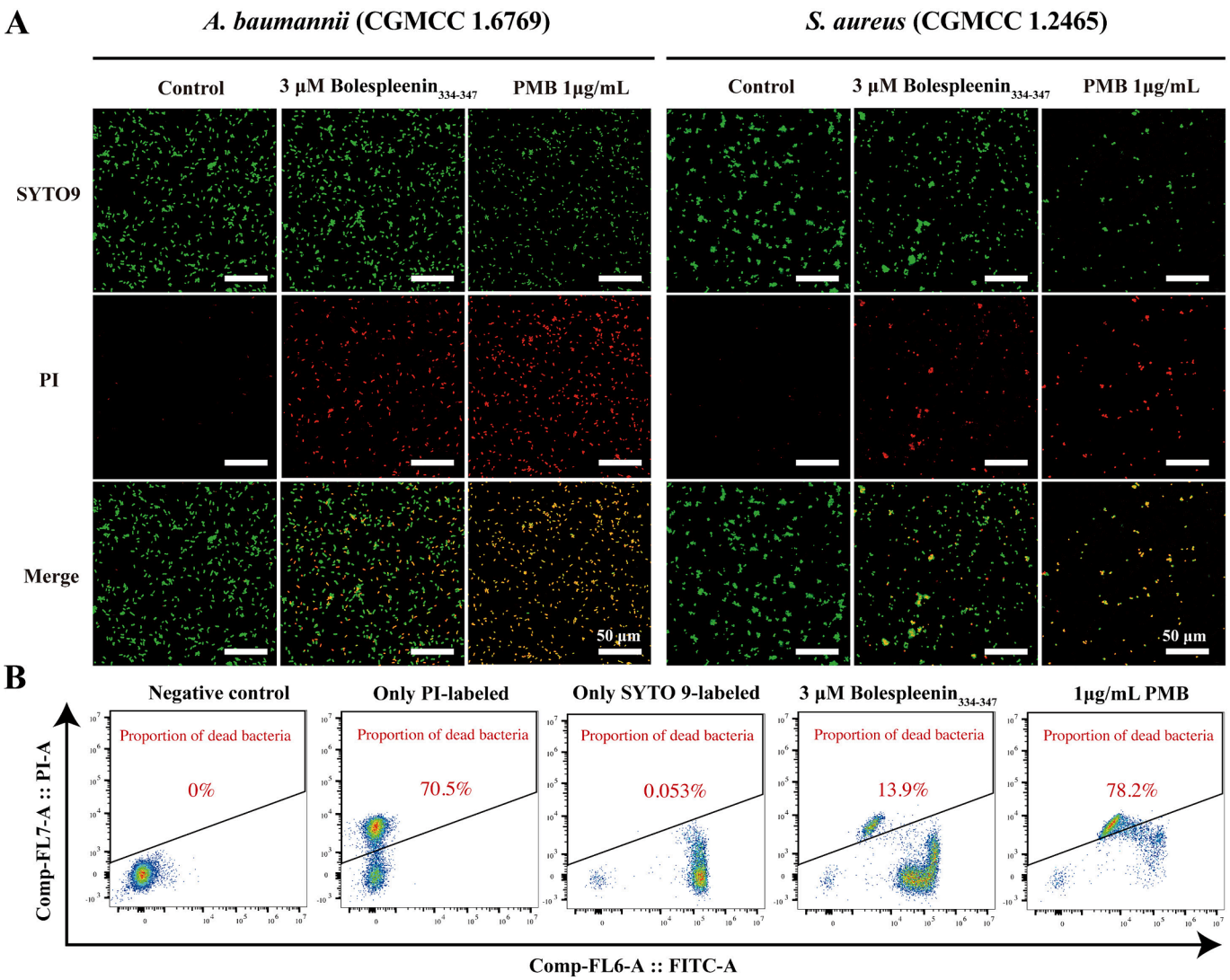


**Fig. 6. Changes in bacterial inner membrane permeability after Bolespleenin$_{334-347}$ treatment.** (A) SYTO 9 and PI staining of Bolespleenin$_{334-347}$-treated bacteria, visualized using CLSM, with PMB serving as a positive control. (B) Flow cytometry-based quantification of the proportion of live and dead bacteria following Bolespleenin$_{334-347}$ treatment, with PMB as a positive control.

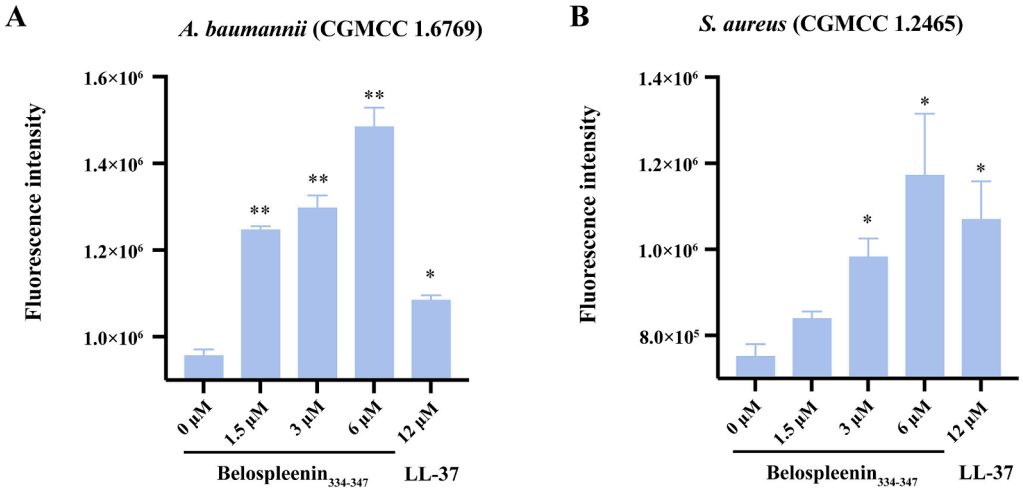


**Fig. 7. The accumulation of ROS levels in bacteria after Bolespleenin$_{334-347}$ treatment.** Changes in endogenous ROS in *A. baumannii* (A) and *S. aureus* (B) after Bolespleenin$_{334-347}$ treatment, which is indirectly indicated by the fluorescence produced through oxidation of DCFH-DA. Data are presented as mean ± standard error of mean (n = 5). Statistical analysis was conducted through one-way ANOVA followed by the Dunnett post hoc test. * $P < 0.05$, ** $P < 0.01$.

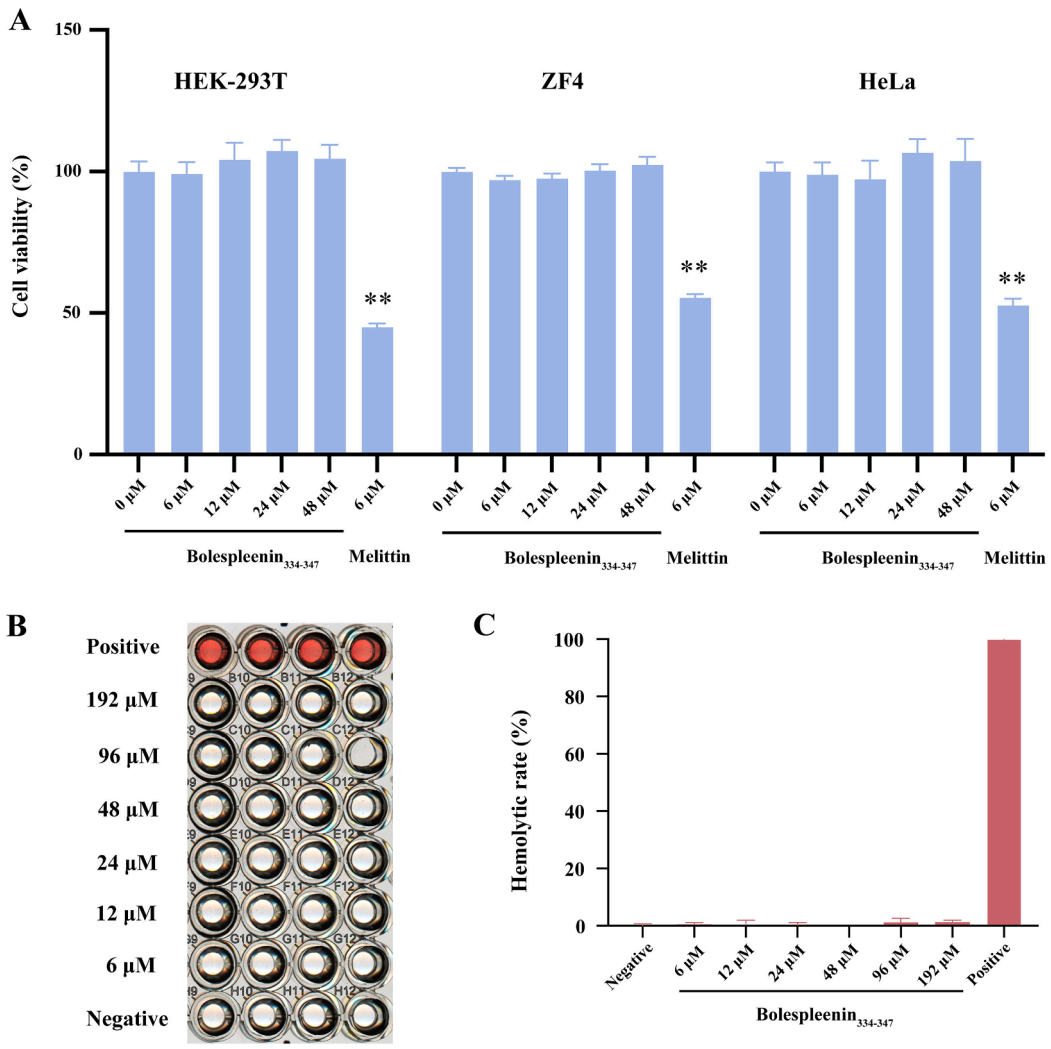


**Fig. 8. *In vitro* cytotoxicity and hemolytic activity of Bolespleenin$_{334-347}$.** (A) The cytotoxicity of Bolespleenin$_{334-347}$ was assessed by MTS-PMS assay on the three subject cells, and no significant toxicity was observed in the concentration range of 0 to 48 μM, in contrast to 6 μM Melittin which significantly inhibited cell proliferation and exhibited significant cytotoxicity. Data are presented as mean ± standard error of mean (n = 5). Statistical analysis was conducted through one-way ANOVA followed by the Dunnett post hoc test. ** $P < 0.01$; (B) and (C) Hemolytic activity of Bolespleenin$_{334-347}$ on mouse erythrocytes. 0.9 % saline was used as a negative control and 0.1 % Triton X-100/saline was used as a positive control.

antibiotics, making it difficult to achieve an effective bactericidal concentration internally, leading to resistance [68]. In the present study, the bactericidal kinetics of Bolespleenin$_{334-347}$ demonstrated that it is highly effective in killing planktonic bacteria, and can rapidly eliminate bacteria in the planktonic phase, thus limiting further development of bacterial biofilms. It is worth noting that antibiotic-resistant bacteria often play a crucial role in the formation of biofilms (insensitive to therapeutic concentrations) [69]. The non-single-target membrane disruption mechanism of action of AMPs limits the development of bacterial resistance due to target mutations [70]. This is a key advantage of Bolespleenin$_{334-347}$ over conventional antibiotics in inhibiting biofilm formation. In addition, several AMPs have been reported to exert anti-biofilm effects by affecting genes involved in biofilm formation, an overlapping anti-biofilm mechanism of AMPs, including the down-regulation of membrane-associated genes responsible for biofilm formation [71], such as the significant down-regulation of *P. aeruginosa rhlI*, *rhlR*, *lasI*, and *lasR* genes by the synthetic peptide WLBU2 [72], and the significant down-regulation of *A. baumannii CsuE*, *BfmR*, *BfmS*, *AbaI* and *Bap* gene expression by the synthetic peptide Cec4 [73]. This regulatory mechanism is dependent on the membrane-interacting activity of the peptide, and Bolespleenin$_{334-347}$, with its strong membrane-interacting activity, is consistent with this overlapping mechanism, and its anti-biofilm investigation will be an essential topic for subsequent research.

The diverse amino acid compositions and structures of AMPs make them less susceptible to develop bacterial drug resistance. However, their activity, stability and toxicity vary to some extent [74,75]. In general, the activity of AMPs is significantly affected by high concentrations of sodium [76,77]. The toxicity of some cationic peptides also greatly limits their application, such as Melittin, which has antimicrobial activity, however, it is significantly toxic to mammalian cells, but this characteristic has also been used in anti-cancer research [78]. In this study, the stability and safety of Bolespleenin$_{334-347}$ were further evaluated. The results showed that high temperature treatment did not affect the activity of Bolespleenin$_{334-347}$. In addition, the antibacterial activity of Bolespleenin$_{334-347}$ was not significantly affected at a sodium concentration of 120 mM. When the sodium concentration was as high as 160 mM, the activity was somewhat weakened, but it was still able to reduce the number of viable bacteria by more than three orders of magnitude, suggesting that Bolespleenin$_{334-347}$ was well tolerated by sodium ions. In the safety evaluation, Bolespleenin$_{334-347}$ did not show significant toxic effects on either cell at the tested concentration (up to 48 μM). In contrast, the positive peptide control Melittin showed significant toxicity at a concentration of only 6 μM. Further evaluation of

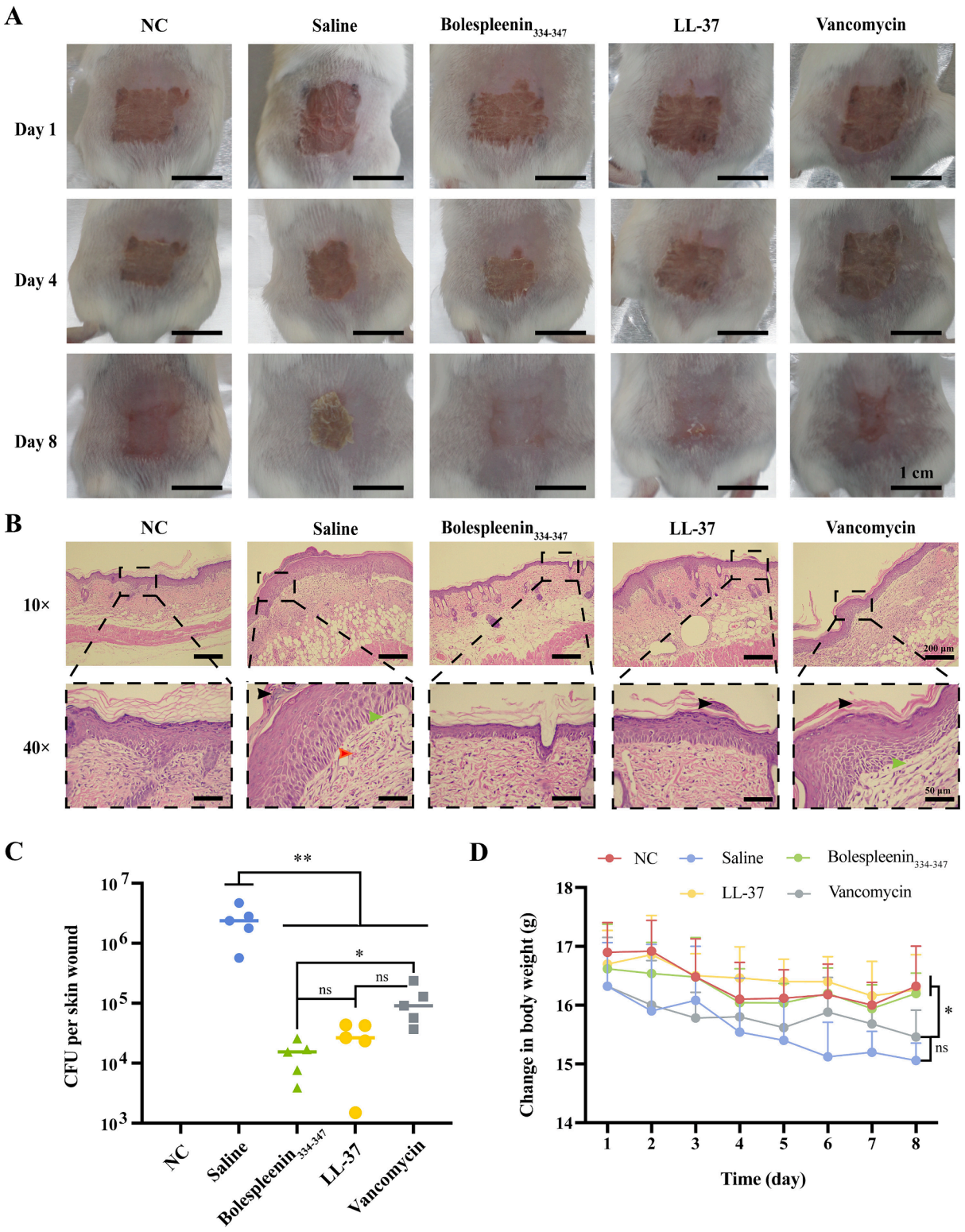


**Fig. 9. Bolespleenin$_{334-347}$ treatment significantly ameliorated MRSA-induced superficial skin infections in mice.** (A) The progression of superficial skin wound healing in MRSA-infected mice was photographed and documented on days 1, 4, and 8. (B) Pathological sections of wound tissue on day 8 were stained with HE. (C) Wound tissue was homogenized and diluted for plate counts to analyze bacterial load. (D) Daily monitoring of mice body weight during drug administration following anesthesia, with changes in body weight recorded over an 8-day period. Data are presented as means ± standard deviations (n = 5). Statistical analysis was conducted through one-way ANOVA followed by the Dunnett post hoc test. * $P < 0.05$, ** $P < 0.01$.

the hemolytic activity of Bolespleenin$_{334-347}$ in mouse erythrocytes showed that no significant hemolysis was observed up to a concentration of 192 μM. It is generally accepted that the cell membranes contain a higher proportion of neutral phospholipids (e.g., phosphatidylcholine or sphingomyelin) than bacterial membranes, with the majority of their negatively charged phospholipids (phosphatidylserine) located in the bilayer cytoplasmic leaflets [76]. In addition, the rigidity of the cell membrane is enhanced by the presence of cholesterol [79]. It is worth mentioning that differences in membrane composition and structure may be important factors in the selectivity of Bolespleenin$_{334-347}$. Taken together, these results indicated that Bolespleenin$_{334-347}$ has good stability and biocompatibility.

*S. aureus* is a common pathogen of superficial skin tissue infections in humans, of which about 59 % of cases are caused by MRSA [9]. Given that Bolespleenin$_{334-347}$ had potent antibacterial activity, and does not readily induce bacterial resistance, it is hypothesized that it may be effective against clinically resistant bacteria. To evaluate the anti-infective potential of Bolespleenin$_{334-347}$, we established a mouse model of MRSA-induced superficial skin infection and compared the efficacy of Bolespleenin$_{334-347}$ with LL-37 and vancomycin. The results demonstrated that all of them significantly reduced the wound bacterial load compared to the control group, but the residual bacterial load in vancomycin-treated wound was significantly higher than that of Bolespleenin$_{334-347}$. Although vancomycin is a first-line agent for the treatment of MRSA, its slower bactericidal rate and poorer tissue penetration demonstrated its limitations in topical therapy [80]. According to our observations, histopathological sections confirmed that wound healing rate with Bolespleenin$_{334-347}$ was superior to those with vancomycin and LL-37, which was partly attributed to the effective wound bacterial clearance.

In addition, AMPs, including LL-37, may promote healing through their chemotactic properties (recruitment of immune cells, keratinocytes) or by promoting angiogenesis [81]. Severe localized skin infections can lead to invasive disease, including endocarditis, osteomyelitis, deep tissue abscesses, sepsis, and pneumonia [4]. Prompt and effective treatment of superficial skin infections is essential to reduce the risk of invasive disease. The efficacy of topical treatment with AMPs is well recognized, e.g. in the treatment of foot infections in diabetic patients, Pexiganan, a derivative of manainin, is comparable to oral fluoroquinolones [82]. As reported in our previous study, Scyreptin$_{1-30}$ identified from marine crabs showed superior therapeutic activity to amikacin and imipenem against multi-drug resistant *P. aeruginosa* infections in a scalded wound study [42]. Currently, at least 15 peptides or mimetics are undergoing (or have completed) clinical trials as antimicrobial agents or immunomodulators [83]. AMP, as a novel antimicrobial agent with a unique antimicrobial mechanism, has promising prospects for future applications.

In summary, a novel AMP Bolespleenin$_{334-347}$ was screened from the marine fish mudskipper *B. pectinirostris*, which possessed broad-spectrum antibacterial activity, good thermal stability and sodium ion tolerance. It inhibited the formation of bacterial biofilm and was not likely to induce the development of bacterial resistance. It could effectively inhibit clinically resistant bacteria and showed therapeutic effects superior to LL-37 and vancomycin in a mouse model of MRSA-induced superficial skin infections. Therefore, the mudskipper is a valuable species for AMP mining due to its special living habits, and the present study will provide an ideal anti-infective candidate and enrich the variety of AMPs in marine fishes.

## CRediT authorship contribution statement

**Yuqi Bai:** Writing – original draft, Visualization, Methodology, Investigation, Formal analysis, Data curation. **Weibin Zhang:** Methodology, Investigation. **Wenbin Zheng:** Methodology, Investigation. **Xin-Zhan Meng:** Investigation. **Yingyi Duan:** Investigation. **Chang Zhang:** Investigation. **Fangyi Chen:** Writing – review & editing, Project administration, Funding acquisition. **Ke-Jian Wang:** Writing – review & editing, Project administration, Funding acquisition.

## Declaration of competing interest

The authors declare that they have no known competing financial interests or personal relationships that could have appeared to influence the work reported in this paper.

## Data availability

Data will be made available on request.

## Acknowledgments

This study was supported by grant 42376089/41806162 from the National Natural Science Foundation of China; grant 2021 J05008 from the Natural Science Foundation of Fujian Province, China; grant FJHY-YYKJ-2024-2-3 and FJHY-YYKJ-2022-1-14 from Fujian Ocean and Fisheries Bureau; grant FOCAL2023-0207 from Fujian Ocean Synergy Alliance (FOCAL) and grant 22CZP002HJ08 from Xiamen Ocean Development Bureau, and grant Z20220743 from Pingtan Research Institute of Xiamen University. We thank laboratory engineers Huiyun Chen, Hui Peng, Zhiyong Lin, Hua Hao and Ming Xiong for providing technical assistance.

## References

[1] T.F. Barlam, S.E. Cosgrove, L.M. Abbo, C. MacDougall, A.N. Schuetz, E.J. Septimus, A. Srinivasan, T.H. Dellit, Y.T. Falck-Ytter, N.O. Fishman, C.W. Hamilton, T. C. Jenkins, P.A. Lipsett, P.N. Malani, L.S. May, G.J. Moran, M.M. Neuhauser, J. G. Newland, C.A. Ohl, M.H. Samore, S.K. Seo, K.K. Trivedi, Implementing an antibiotic stewardship program: guidelines by the infectious diseases society of america and the society for healthcare epidemiology of America, Clin. Infect. Dis. 62 (10) (2016) 1197–1202.

[2] M.I. Hutchings, A.W. Truman, B. Wilkinson, Antibiotics: past, present and future, Curr. Opin. Microbiol. 51 (2019) 72–80.

[3] S.F. Nadeem, U.F. Gohar, S.F. Tahir, H. Mukhtar, S. Pornpukdeewattana, P. Nukthamna, A.M.M. Ali, S.C.B. Bavisetty, S. Massa, Antimicrobial resistance: more than 70 years of war between humans and bacteria, Crit. Rev. Microbiol. 46 (5) (2020) 578–599.

[4] R. Olaniyi, C. Pozzi, L. Grimaldi, F. Bagnoli, *Staphylococcus aureus*-associated skin and soft tissue infections: anatomical localization, epidemiology, therapy and potential prophylaxis, Curr. Top. Microbiol. Immunol. 409 (2017) 199–227.

[5] V. Vella, I. Galgani, L. Polito, A.K. Arora, C.B. Creech, M.Z. David, F.D. Lowy, N. Macesic, J.P. Ridgway, A.C. Uhlemann, F. Bagnoli, *Staphylococcus aureus* skin and soft tissue infection recurrence rates in outpatients: a retrospective database study at 3 US medical centers, Clin. Infect. Dis. 73 (5) (2021) E1045–E1053.

[6] L. Tognetti, C. Martinelli, S. Berti, J. Hercogova, T. Lotti, F. Leoncini, S. Moretti, Bacterial skin and soft tissue infections: review of the epidemiology, microbiology, aetiopathogenesis and treatment: a collaboration between dermatologists and infectivologists, J. Eur. Acad. Dermatol. Venereol. 26 (8) (2012) 931–941.

[7] C.M. Kao, S.A. Fritz, Infection prevention—how can we prevent transmission of community-onset methicillin-resistant *Staphylococcus aureus*? Clin. Microbiol. Infect. (2024).

[8] M.Z. David, R.S. Daum, Community-associated methicillin-resistant *Staphylococcus aureus*: epidemiology and clinical consequences of an emerging epidemic, Clin. Microbiol. Rev. 23 (3) (2010) 616-+.

[9] G.J. Moran, A. Krishnadasan, R.J. Gorwitz, G.E. Fosheim, L.K. McDougal, R. B. Carey, D.A. Talan, E.I.N.S. Grp, S. Methicillin-resistant, *aureus* infections among patients in the emergency department, N. Engl. J. Med. 355 (7) (2006) 666–674.

[10] D.A. Williamson, G.P. Carter, B.P. Howden, Current and emerging topical antibacterials and antiseptics: agents, action, and resistance patterns, Clin. Microbiol. Rev. 30 (3) (2017) 827–860.

[11] C.V. Lundberg, N. Frimodt-Moller, Efficacy of topical and systemic antibiotic treatment of meticillin-resistant *Staphylococcus aureus* in a murine superficial skin wound infection model, Int. J. Antimicrob. Agents 42 (3) (2013) 272–275.

[12] M.D. Johnson, C.F. Decker, Antimicrobial agents in treatment of MRSA infections, Dis. Mon. 54 (12) (2008) 793–800.

[13] N.A. Turner, B.K. Sharma-Kuinkel, S.A. Maskarinec, E.M. Eichenberger, P.P. Shah, M. Carugati, T.L. Holland, V.G. Fowler, Methicillin-resistant *Staphylococcus aureus*: an overview of basic and clinical research, Nat. Rev. Microbiol. 17 (4) (2019) 203–218.

[14] K.U. Jansen, W.C. Gruber, R. Simon, J. Wassil, A.S. Anderson, The impact of human vaccines on bacterial antimicrobial resistance a review, Environ. Chem. Lett. 19 (6) (2021) 4031–4062.

[15] G.S. Becker, Antibiotic use in agriculture: background and legislation, Congress. Res. Ser. (2010).
[16] J. Garau, Impact of antibiotic restrictions: the ethical perspective, Clin. Microbiol. Infect. 12 (2006) 16–24.
[17] H.X. Luong, T.T. Thanh, T.H. Tran, Antimicrobial peptides - advances in development of therapeutic applications, Life Sci. 260 (2020).
[18] D. Ciumac, H.N. Gong, X.Z. Hu, J.R. Lu, Membrane targeting cationic antimicrobial peptides, J. Colloid Interface Sci. 537 (2019) 163–185.
[19] C. Kao, X.Y. Lin, G.H. Yi, Y.L. Zhang, D.A. Rowe-Magnus, K. Bush, Cathelicidin antimicrobial peptides with reduced activation of toll-like receptor signaling have potent bactericidal activity against colistin-resistant bacteria, MBio 7 (5) (2016).
[20] F. Semple, J.R. Dorin, β-defensins: multifunctional modulators of infection, inflammation and more? J. Innate Immun. 4 (4) (2012) 337–348.
[21] L.J. Zhang, R.L. Gallo, Antimicrobial peptides, Curr. Biol. 26 (1) (2016) R14–R19.
[22] M. Mahlapuu, J. Håkansson, L. Ringstad, C. Björn, Antimicrobial peptides : an emerging category of therapeutic agents, Front. Cell. Infect. Microbiol. 6 (2016).
[23] A. Pfalzgraff, K. Brandenburg, G. Weindl, Antimicrobial peptides and their therapeutic potential for bacterial skin infections and wounds, Front. Pharmacol. 9 (2018).
[24] T.T. Odunitan, A.O. Oyaronbi, F.A. Adebayo, P.A. Adekoyeni, B.T. Apanisile, T. D. Oladunni, O.A. Saibu, Antimicrobial peptides: a novel and promising arsenal against methicillin-resistant *Staphylococcus aureus* (MRSA) infections, Pharm. Sci. Adv. (2023) 100034.
[25] B.C. Lin, A.D. Hung, R. Li, A. Barlow, W. Singleton, T. Matthyssen, M.A.D. Sani, M. A. Hossain, J. Wade, N.M. O'Brien-Simpson, W.Y. Li, Systematic comparison of activity and mechanism of antimicrobial peptides against nosocomial pathogens, Eur. J. Med. Chem. 231 (2022).
[26] E. Ciandrini, G. Morroni, D. Arzeni, W. Kamysz, D. Neubauer, E. Kamysz, O. Cirioni, L. Brescini, W. Baffone, R. Campana, Antimicrobial activity of different antimicrobial peptides (AMPs) against clinical methicillin-resistant *Staphylococcus aureus* (MRSA), Curr. Top. Med. Chem. 18 (24) (2018) 2116–2126.
[27] F. Costa, C. Teixeira, P. Gomes, M.C.L. Martins, Clinical Application of AMPs, Advances in Experimental Medicine and Biology 1117 (2019) 281–298.
[28] J. Fox, Antimicrobial peptides stage a comeback (vol 31, pg 379, 2013), Nat. Biotechnol. 31 (12) (2013) 1066.
[29] W.Y. Li, F. Separovic, N.M. O'Brien-Simpson, J.D. Wade, Chemically modified and conjugated antimicrobial peptides against superbugs, Chem. Soc. Rev. 50 (8) (2021) 4932–4973.
[30] Y.J. Han, M.L. Zhang, R. Lai, Z.Y. Zhang, Chemical modifications to increase the therapeutic potential of antimicrobial peptides, Peptides 146 (2021).
[31] P.Y. Chen, T. Ye, C.Y. Li, P. Praveen, Z.L. Hu, W.Y. Li, C.J. Shang, Embracing the era of antimicrobial peptides with marine organisms, Nat. Prod. Rep. 41 (3) (2024).
[32] S.C. Wang, L.M. Fan, H.Y. Pan, Y.Y. Li, Y. Qiu, Y.M. Lu, Antimicrobial peptides from marine animals: sources, structures, mechanisms and the potential for drug development, Front. Mar. Sci. 9 (2023).
[33] H.N. Huang, V. Rajanbabu, C.Y. Pan, Y.L. Chan, C.J. Wu, J.Y. Chen, Use of the antimicrobial peptide Epinecidin-1 to protect against MRSA infection in mice with skin injuries, Biomaterials 34 (38) (2013) 10319–10327.
[34] P.K. Hazam, J.Y. Chen, Therapeutic utility of the antimicrobial peptide Tilapia Piscidin 4 (TP4), Aquacult. Rep. 17 (2020).
[35] J.S. Nelson, T.C. Grande, M.V. Wilson, Fishes of the World, John Wiley & Sons, 2016.
[36] Y.H. Yi, X.X. You, C. Bian, S.X. Chen, Z. Lv, L.M. Qiu, Q. Shi, High-throughput identification of antimicrobial peptides from amphibious mudskippers, Mar. Drugs 15 (11) (2017).
[37] D.P. Zhu, F.Y. Chen, Y.C. Chen, H. Peng, K.J. Wang, The long-term effect of a nine amino-acid antimicrobial peptide AS-hepc3$_{(48-56)}$ Against *Pseudomonas aeruginosa* with no detectable resistance, Front. Cell. Infect. Microbiol. 11 (2021).
[38] X.F. Wang, X. Hong, F.Y. Chen, K.J. Wang, A truncated peptide Spgillcin$_{177-189}$ derived from mud crab Scylla paramamosain exerting multiple antibacterial activities, Front. Cell. Infect. Microbiol. 12 (2022).
[39] J. Liu, F.Y. Chen, X.F. Wang, H. Peng, H. Zhang, K.J. Wang, The synergistic effect of mud crab antimicrobial peptides sphistin and Sph$_{12-38}$ with antibiotics azithromycin and rifampicin enhances bactericidal activity against *pseudomonas aeruginosa*, Front. Cell. Infect. Microbiol. 10 (2020).
[40] Y. Yang, F. Chen, H.Y. Chen, H. Peng, H. Hao, K.J. Wang, A novel antimicrobial peptide Scyreprocin from mud crab *Scylla paramamosain* showing potent antifungal and anti-biofilm activity, Front. Microbiol. 11 (2020) 1589.
[41] A. Farkas, G. Maroti, A. Kereszt, E. Kondorosi, Comparative analysis of the bacterial membrane disruption effect of two natural plant antimicrobial peptides, Front. Microbiol. 8 (2017) 51.
[42] W.B. Zhang, Z. An, Y.Q. Bai, Y. Zhou, F.Y. Chen, K.J. Wang, A novel antimicrobial peptide Scyreptin1-30 from *Scylla paramamosain* exhibiting potential therapy of *Pseudomonas aeruginosa* early infection in a mouse burn wound model, Biochem. Pharmacol. 218 (2023).
[43] E. Kugelberg, T. Norstrom, T.K. Petersen, T. Duvold, D.I. Andersson, D. Hughes, Establishment of a superficial skin infection model in mice by using *Staphylococcus aureus* and *Streptococcus pyogenes*, Antimicrob. Agents Chemother. 49 (8) (2005) 3435–3441.
[44] M. Krishnan, J. Choi, A. Jang, S. Choi, J. Yeon, M. Jang, Y. Lee, K. Son, S.Y. Shin, M.S. Jeong, Y. Kim, Molecular mechanism underlying the TLR4 antagonistic and antiseptic activities of papiliocin, an insect innate immune response molecule, Proceedings of the National Academy of Sciences 119(10) (2022).
[45] A. Rajput, A. Thakur, S. Sharma, M. Kumar, aBiofilm: a resource of anti-biofilm agents and their potential implications in targeting antibiotic drug resistance, Nucleic Acids Res. 46 (D1) (2018) D894–D900.
[46] P. Gallagher, S. Baker, Developing new therapeutic approaches for treating infections caused by multi-drug resistant *Acinetobacter baumannii*: *acinetobacter baumannii* therapeutics, J. Infect. 81 (6) (2020) 857–861.
[47] M. Palusinska-Szysz, M. Jurak, N. Gisch, F. Waldow, N. Zehethofer, C. Nehls, D. Schwudke, P. Koper, A. Mazur, The human LL-37 peptide exerts antimicrobial activity against *Legionella micdadei* interacting with membrane phospholipids, Biochim. Biophys. Acta (BBA)-Mol. Cell Biol. Lipids 1867 (6) (2022).
[48] N. Malanovic, K. Lohner, Gram-positive bacterial cell envelopes: the impact on the activity of antimicrobial peptides, Biochim. Biophys. Acta (BBA)-Biomembr. 1858 (5) (2016) 936–946.
[49] A. Mourenza, J.A. Gil, L.M. Mateos, M. Letek, Oxidative stress-generating antimicrobials, a novel strategy to overcome antibacterial resistance, Antioxidants-Basel 9 (5) (2020).
[50] A.M. Lima, M.I.G. Azevedo, L.M. Sousa, N.S. Oliveira, C.R. Andrade, C.D.T. Freitas, P.F.N. Souza, Plant antimicrobial peptides: an overview about classification, toxicity and clinical applications, Int. J. Biol. Macromol. 214 (2022) 10–21.
[51] G. Wang, X. Li, Z. Wang, APD3: the antimicrobial peptide database as a tool for research and education, Nucleic Acids Res. 44 (D1) (2016) D1087–D1093.
[52] X.X. You, C. Bian, Q.J. Zan, X. Xu, X. Liu, J.M. Chen, J.T. Wang, Y. Qiu, W.J. Li, X. H. Zhang, Y. Sun, S.X. Chen, W.S. Hong, Y.X. Li, S.F. Cheng, G.Y. Fan, C.C. Shi, J. Liang, Y.T. Tang, C.Y. Yang, Z.Q. Ruan, J. Bai, C. Peng, Q. Mu, J. Lu, M.J. Fan, S. Yang, Z.Y. Huang, X.T. Jiang, X.D. Fang, G.J. Zhang, Y. Zhang, G. Polgar, H. Yu, J. Li, Z.J. Liu, G.Q. Zhang, V. Ravi, S.L. Coon, J. Wang, H.M. Yang, B. Venkatesh, J. Wang, Q. Shi, Mudskipper genomes provide insights into the terrestrial adaptation of amphibious fishes, Nat. Commun. 5 (2014).
[53] R. Gibson, Intertidal fishes, Encycl. Ocean Sci. 3 (2001) 1348–1354.
[54] R. Bruno, C. Boidin-Wichlacz, O. Melnyk, D. Zeppilli, C. Landon, F. Thomas, M. A. Cambon, M. Lafond, K. Mabrouk, F. Massol, S. Hourdez, M. Maresca, D. Jollivet, A. Tasiemski, The diversification of the antimicrobial peptides from marine worms is driven by environmental conditions, Sci. Total Environ. 879 (2023).
[55] Z. Li, W.S. Hong, H.T. Qiu, T.Z. Yu, M.S. Yang, X.X. You, S.X. Chen, Cloning and expression of two hepcidin genes in the mudskipper (*Boleophthalmus pectinirostris*) provides insights into their roles in male reproductive immunity, Fish Shellfish Immunol. 56 (2016) 239–247.
[56] A. Alesci, G. Capillo, D.M. Mokhtar, A. Fumia, R. D'Angelo, P. Lo Cascio, M. Albano, M.C. Guerrera, R.K.A. Sayed, N. Spanò, S. Pergolizzi, E.R. Lauriano, Expression of antimicrobic peptide piscidin1 in gills mast cells of giant mudskipper *periophthalmodon schlosseri* (Pallas, 1770), Int. J. Mol. Sci. 23 (22) (2022).
[57] V. Teixeira, M.J. Feio, M. Bastos, Role of lipids in the interaction of antimicrobial peptides with membranes, Prog. Lipid Res. 51 (2) (2012) 149–177.
[58] M.A. Sani, F. Separovic, How membrane-active peptides get into lipid membranes, Acc. Chem. Res. 49 (6) (2016) 1130–1138.
[59] K.J. Cutrona, B.A. Kaufman, D.M. Figueroa, D.E. Elmore, Role of arginine and lysine in the antimicrobial mechanism of histone-derived antimicrobial peptides, FEBS Lett. 589 (24) (2015) 3915–3920.
[60] A. Mollica, G. Macedonio, A. Stefanucci, R. Costante, S. Carradori, V. Cataldi, M. Di Giulio, L. Cellini, R. Silvestri, C. Giordano, A. Scipioni, S. Morosetti, P. Punzi, S. Mirzaie, Arginine- and lysine-rich peptides: synthesis, characterization and antimicrobial activity, Lett. Drug Des. Discovery 15 (3) (2018) 220–226.
[61] B. Lin, A. Hung, W. Singleton, K.K. Darmawan, R. Moses, B. Yao, H. Wu, A. Barlow, M.A. Sani, A.J. Sloan, The effect of tailing lipidation on the bioactivity of antimicrobial peptides and their aggregation tendency: special issue: emerging investigators, Aggregate 4 (4) (2023) e329.
[62] L.B. Li, I. Vorobyov, T.W. Allen, The different interactions of lysine and arginine side chains with lipid membranes, J. Phys. Chem. B 117 (40) (2013) 11906–11920.
[63] Y. Takechi, H. Yoshii, M. Tanaka, T. Kawakami, S. Aimoto, H. Saito, Physicochemical mechanism for the enhanced ability of lipid membrane penetration of polyarginine, Langmuir 27 (11) (2011) 7099–7107.
[64] M.N. Melo, R. Ferre, M.A.R.B. Castanho, Antimicrobial peptides: linking partition, activity and high membrane-bound concentrations, Nat. Rev. Microbiol. 7 (3) (2009) 245–250.
[65] A.T. Dharmaraja, Role of reactive oxygen species (ROS) in therapeutics and drug resistance in cancer and bacteria, J. Med. Chem. 60 (8) (2017) 3221–3240.
[66] F. Vatansever, W.C.M.A. de Melo, P. Avci, D. Vecchio, M. Sadasivam, A. Gupta, R. Chandran, M. Karimi, N.A. Parizotto, R. Yin, G.P. Tegos, M.R. Hamblin, Antimicrobial strategies centered around reactive oxygen species - bactericidal antibiotics, photodynamic therapy, and beyond, FEMS Microbiol. Rev. 37 (6) (2013) 955–989.
[67] C.A. Fux, J.W. Costerton, P.S. Stewart, P. Stoodley, Survival strategies of infectious biofilms, Trends Microbiol. 13 (1) (2005) 34–40.
[68] L. Segev-Zarko, R. Saar-Dover, V. Brumfeld, M.L. Mangoni, Y. Shai, Mechanisms of biofilm inhibition and degradation by antimicrobial peptides, Biochem. J 468 (2015) 259–270.
[69] R.V. Sionov, D. Steinberg, Targeting the holy triangle of quorum sensing, biofilm formation, and antibiotic resistance in pathogenic bacteria, Microorganisms 10 (6) (2022).
[70] A. Mor, Peptide-based antibiotics: a potential answer to raging antimicrobial resistance, Drug Dev. Res. 50 (3–4) (2000) 440–447.
[71] M. Yasir, M.D.P. Willcox, D. Dutta, Action of antimicrobial peptides against bacterial biofilms, Materials 11 (12) (2018).
[72] S. Masihzadeh, M. Amin, Z. Farshadzadeh, In vitro and in vivo antibiofilm activity of the synthetic antimicrobial peptide WLBU2 against multiple drug resistant *Pseudomonas aeruginosa* strains, BMC Microbiol. 23 (1) (2023).

[73] W. Liu, Z. Wu, C. Mao, G. Guo, Z. Zeng, Y. Fei, S. Wan, J. Peng, J. Wu, Antimicrobial peptide cec4 eradicates the bacteria of clinical carbapenem-resistant *acinetobacter baumannii* biofilm, Front. Microbiol. 11 (2020) 1532.
[74] P. Kumar, J.N. Kizhakkedathu, S.K. Straus, Antimicrobial peptides: diversity, mechanism of action and strategies to improve the activity and biocompatibility in vivo, Biomolecules 8 (1) (2018).
[75] T.A. Stone, G.B. Cole, D. Ravamehr-Lake, H.Q. Nguyen, F. Khan, S. Sharpe, C. M. Deber, Positive charge patterning and hydrophobicity of membrane-active antimicrobial peptides as determinants of activity toxicity, and pharmacokinetic stability, J. Med. Chem. 62 (13) (2019) 6276–6286.
[76] B.H. Gan, J. Gaynord, S.M. Rowe, T. Deingruber, D.R. Spring, The multifaceted nature of antimicrobial peptides: current synthetic chemistry approaches and future directions, Chem. Soc. Rev. 50 (13) (2021) 7820–7880.
[77] J.J. Smith, S.M. Travis, E.P. Greenberg, M.J. Welsh, Cystic fibrosis airway epithelia fail to kill bacteria because of abnormal airway surface fluid, Cell 85 (2) (1996) 229–236.
[78] G. Gajski, V. Garaj-Vrhovac, Melittin: a lytic peptide with anticancer properties, Environ. Toxicol. Pharmacol. 36 (2) (2013) 697–705.
[79] J.R. Brender, A.J. McHenry, A. Ramamoorthy, Does cholesterol play a role in the bacterial selectivity of antimicrobial peptides? Front. Immunol. 3 (2012).
[80] M.H. Kollef, Limitations of vancomycin in the management of resistant staphylococcal infections, Clin. Infect. Dis. 45 (2007) S191–S195.
[81] K. Bandurska, A. Berdowska, R. Barczynska-Felusiak, P. Krupa, Unique features of human cathelicidin LL-37, Biofactors 41 (5) (2015) 289–300.
[82] B.A. Lipsky, K.J. Holroyd, M. Zasloff, Topical versus systemic antimicrobial therapy for treating mildly infected diabetic foot ulcers: a randomized controlled, double-blinded, multicenter trial of pexiganan cream, Clin. Infect. Dis. 47 (12) (2008) 1537–1545.
[83] C.D. Fjell, J.A. Hiss, R.E.W. Hancock, G. Schneider, Designing antimicrobial peptides: form follows function, Nat. Rev. Drug Discov. 11 (1) (2012) 37–51.